

Fig. S.1. Structural formula of raw material of CDs-NAC and CDs-GSH containing CA, L-NAC and GSH.

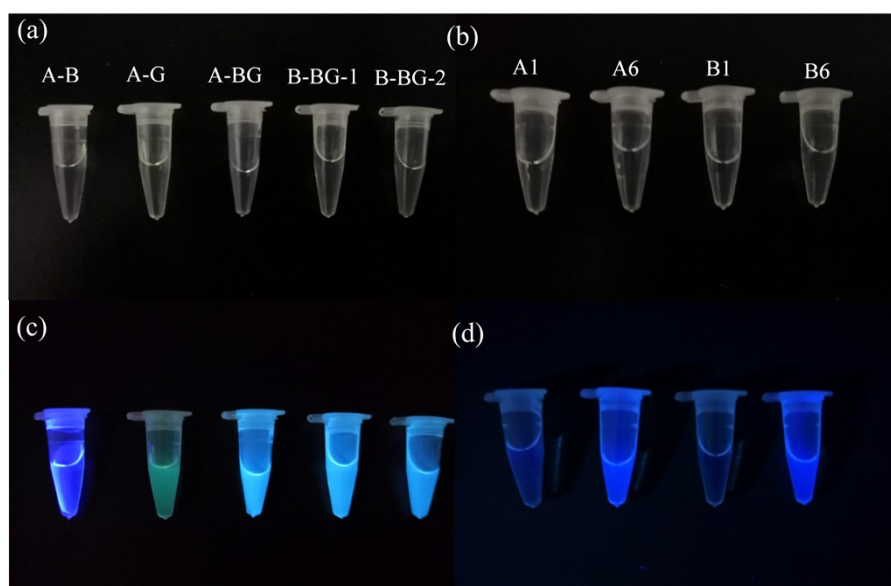


Fig. S.2. (a) Pictures of the separated fluorophores from CDs-NAC and CDs-GSH under white light. (b) Pictures of the first stage and final product of CDs-NAC and CDs-GSH under white light. (c) Pictures of the separated fluorophores from CDs-NAC and CDs-GSH under white 365 nm UV lamplight. (d) Pictures of the first stage and final product of CDs-NAC and CDs-GSH under 365 nm UV lamp.

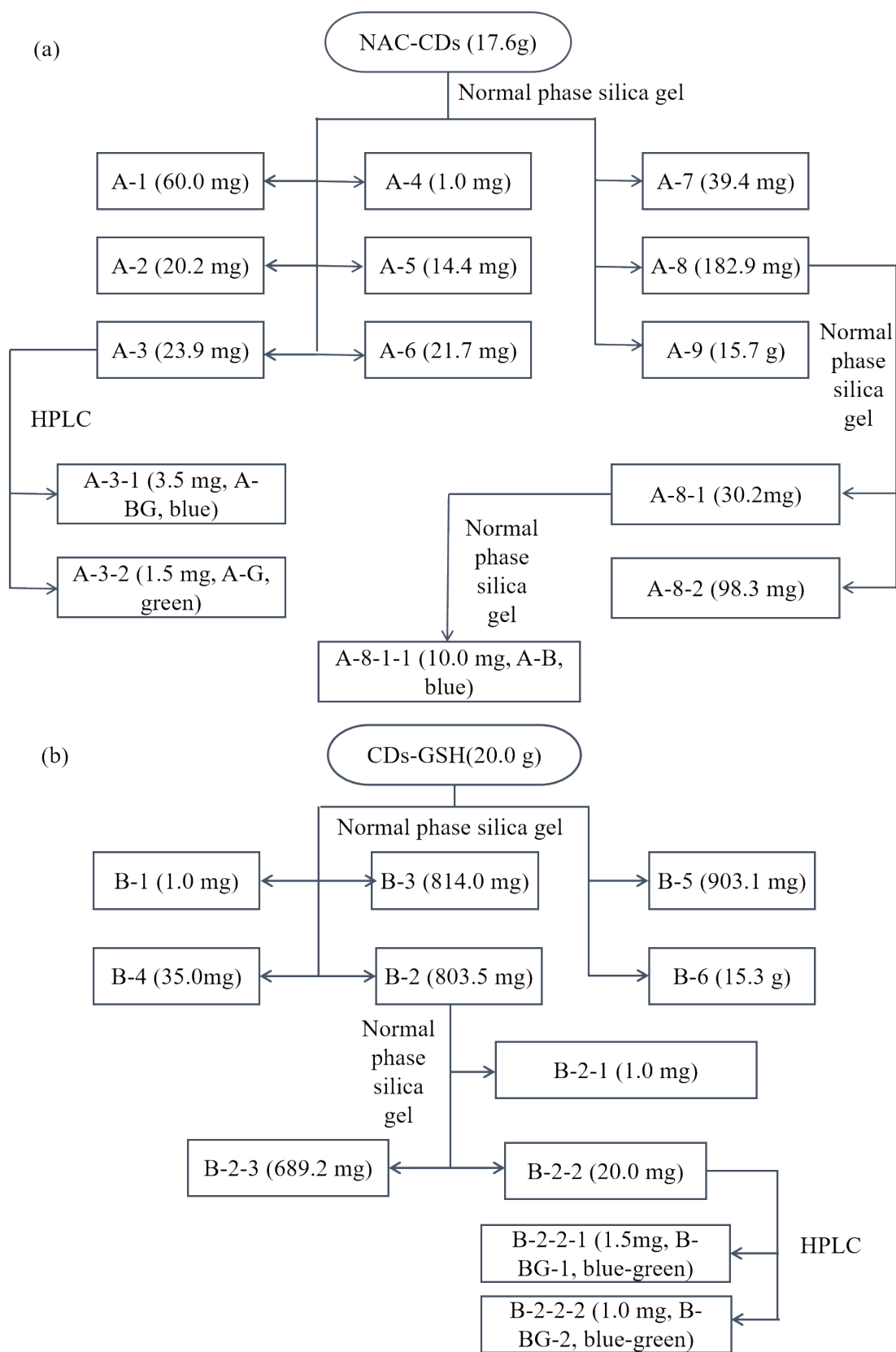


Fig. S.3. Flow chart of separation of (a) CDs-NAC and (b) CDs-GSH.

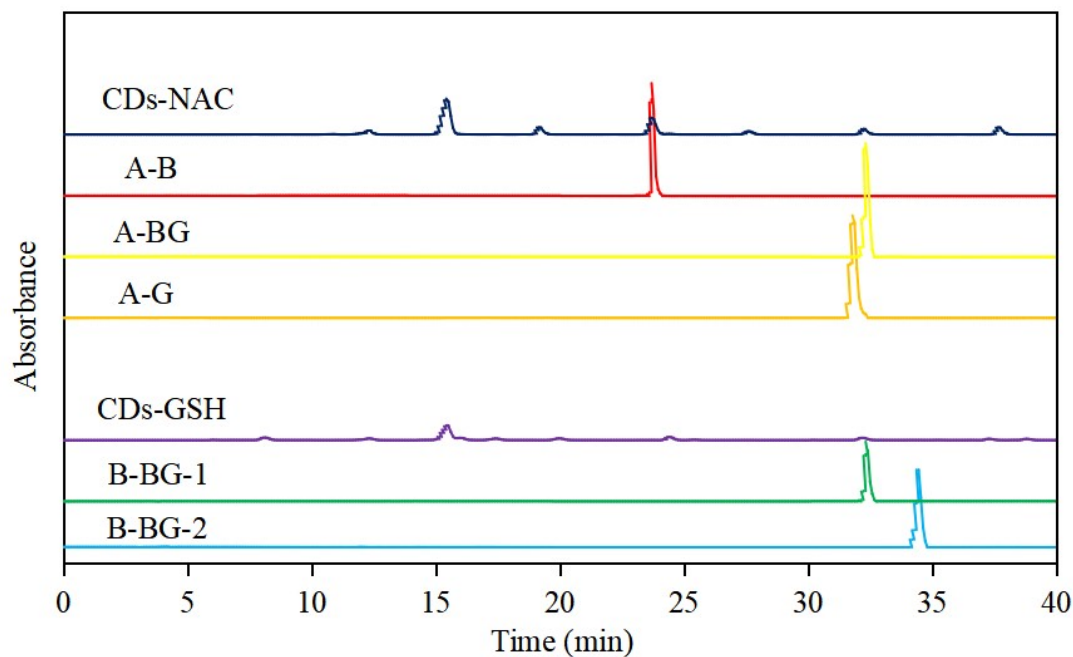
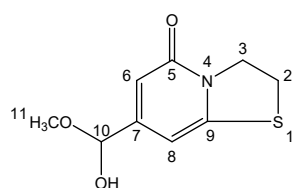


Fig. S.4. the absorption chromatograms of CDs-NAC, CDs-GSH and the separated fluorophores from CDs-NAC and CDs-GSH monitored at 365 nm. All of these were carried out under the same HPLC conditions. Column temperature: 25 °C; Eluent ratio and time: acetonitrile and water were used as two phases and all samples were eluted with acetonitrile whose concentration is from 15% to 55% during 45 min.

The Concrete results of NMR and ESI-HRMS of fluorophores separated from CDs-NAC and CDs-GSH.



5-oxo-2,3-dihydrothiazolo[3,2-a]pyridine-7-carboxylate (A-B).

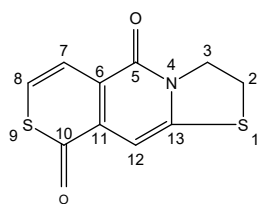
Colorless amorphous powder. ¹H-NMR (600 MHz, CD₃DH-d₄): δ

6.69, 6.70 (2H, d), 4.46 (2H, t, *J*=7.2 Hz), 3.86 (3H, s), 3.53 (2H, t,

J=7.2 Hz); ¹³C-NMR (150 MHz, CD₃DH-d₄): δ 166.2 (C-10), 164.1

(C-5), 152.5 (C-9), 143.5 (C-7), 116.0 (C-6), 100.9 (C-8), 53.6 (C-11), 52.6 (C-3), 29.40 (C-2), ;

HRMS (ESI) [M+H]⁺ C₉H₉N₂O₃S calcd 212.0376, found 212.0380 (Fig. S.5~S.10).

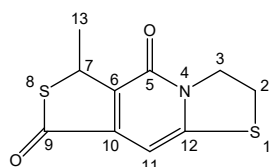


2,3-dihydrothiazolo[3,2-a]thiopyrano[3,4-d] pyridine -5,10-dione (A-G).

Green amorphous powder. ¹H-NMR (600 MHz, CD₃CL-d₃): δ 7.66 (1H,

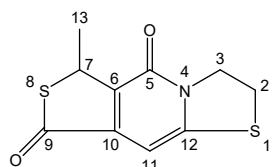
d, 7.2), 7.17 (1H, d, 7.2), 6.86 (1H, s), 4.54 (2H, t, 7.2), 3.46 (2H, t, 7.2);

^{13}C -NMR (600 MHz, $\text{CD}_3\text{CL-d}_3$): 185.2 (C-10), 161.2 (C-5), 147.0 (C-13), 135.0 (C-11), 127.3 (C-6), 126.3 (C-8), 116.9 (C-7), 94.6 (C-12), 51.3 (C-3), 28.6 (C-2); HRMS (ESI) $[\text{M}+\text{H}]^+$ $\text{C}_{10}\text{H}_7\text{H}^+\text{NO}_2\text{S}_2$ calcd 237.9991, found 237.9991 (Fig. S.11~S.16).



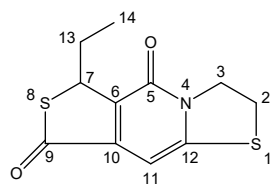
7-methyl-2,3-dihydrothiazolo[3,2-a]-7H-thieno[3,4-d]pyridine-5,9-dione (A-BG).

Light blue amorphous powder. ^1H -NMR (600 MHz, $\text{CD}_3\text{CL-d}_3$): δ 6.415 (1H, s), 4.768 (1H, q, $J=7.2$ Hz), 4.500 (2H, m, $J_1=7.2$ Hz, $J_2=13.2$ Hz), 3.48 (2H, t, $J=7.2$ Hz), 1.78 (3H, d, $J=7.2$ Hz); ^{13}C -NMR (600 MHz, $\text{CD}_3\text{CL-d}_3$): δ 196.1 (C-9), 159.1 (C-5), 150.1 (C-12), 145.8 (C-10), 138.5 (C-6). 93.5 (C-11), 50.7 (C-3), 44.9 (C-7), 29.4 (C-2), 19.8 (C-13); HRMS (ESI) $[\text{M}+\text{H}]^+$ $\text{C}_{10}\text{H}_9\text{H}^+\text{NO}_2\text{S}_2$ calcd 240.0148, found 240.0147 (Fig. S.17~S.22).



7-methyl-2,3-dihydrothiazolo[3,2-a]-7H-thieno[3,4-d]pyridine-5,9-dione (B-BG-1).

Light blue amorphous powder. ^1H -NMR (600 MHz, $\text{CD}_3\text{CL-d}_3$): δ 6.42 (1H, s), 4.77 (1H, q, $J=7.2$ Hz), 4.50 (2H, m, $J_1=7.2$ Hz, $J_2=13.2$ Hz), 3.49 (2H, t, $J=7.2$ Hz), 1.79 (3H, d, $J=7.2$ Hz); ^{13}C -NMR (600 MHz, $\text{CD}_3\text{CL-d}_3$): δ 196.1 (C-9), 159.1 (C-5), 150.1 (C-12), 145.8 (C-10), 138.5 (C-6). 93.5 (C-11), 50.7 (C-3), 44.9 (C-7), 29.4 (C-2), 19.8 (C-13); HRMS (ESI) $[\text{M}+\text{H}]^+$ $\text{C}_{10}\text{H}_9\text{H}^+\text{NO}_2\text{S}_2$ calcd 240.0148, found 240.0147 (Fig. S.23~S.28).



7-ethyl-2,3-dihydrothiazolo[3,2-a]-7H-thieno[3,4-d]pyridine-5,9-dione (B-G-2).

Light blue amorphous powder. ^1H -NMR (600 MHz, $\text{CD}_3\text{CL-d}_3$): δ 6.42 (1H, s), 4.74 (1H, d, $J=9$ Hz), 4.51 (2H, m, $J_1=7.2$ Hz, $J_2=13.8$ Hz), 3.48 (2H, t, $J=7.2$ Hz), 2.59, 1.82 (2H, m), 1.00 (3H, d, $J=7.2$ Hz); ^{13}C -NMR (600 MHz, $\text{CD}_3\text{CL-d}_3$): δ 196.4 (C-9), 159.1 (C-5), 150.0 (C-12), 146.2 (C-10), 137.3 (C-6). 93.6 (C-11), 52.5 (C-3), 50.7 (C-7), 29.3 (C-2), 26.3 (C-13) 12.1 (C-14); HRMS (ESI) $[\text{M}+\text{H}]^+$ $\text{C}_{11}\text{H}_{11}\text{H}^+\text{NO}_2\text{S}_2$ calcd 254.0304, found 254.0303 (Fig. S.29-S.34).

Table 1. The data about ^1H -NMR and ^{13}C -NMR of all fluorophores separated from CDs-NAC and

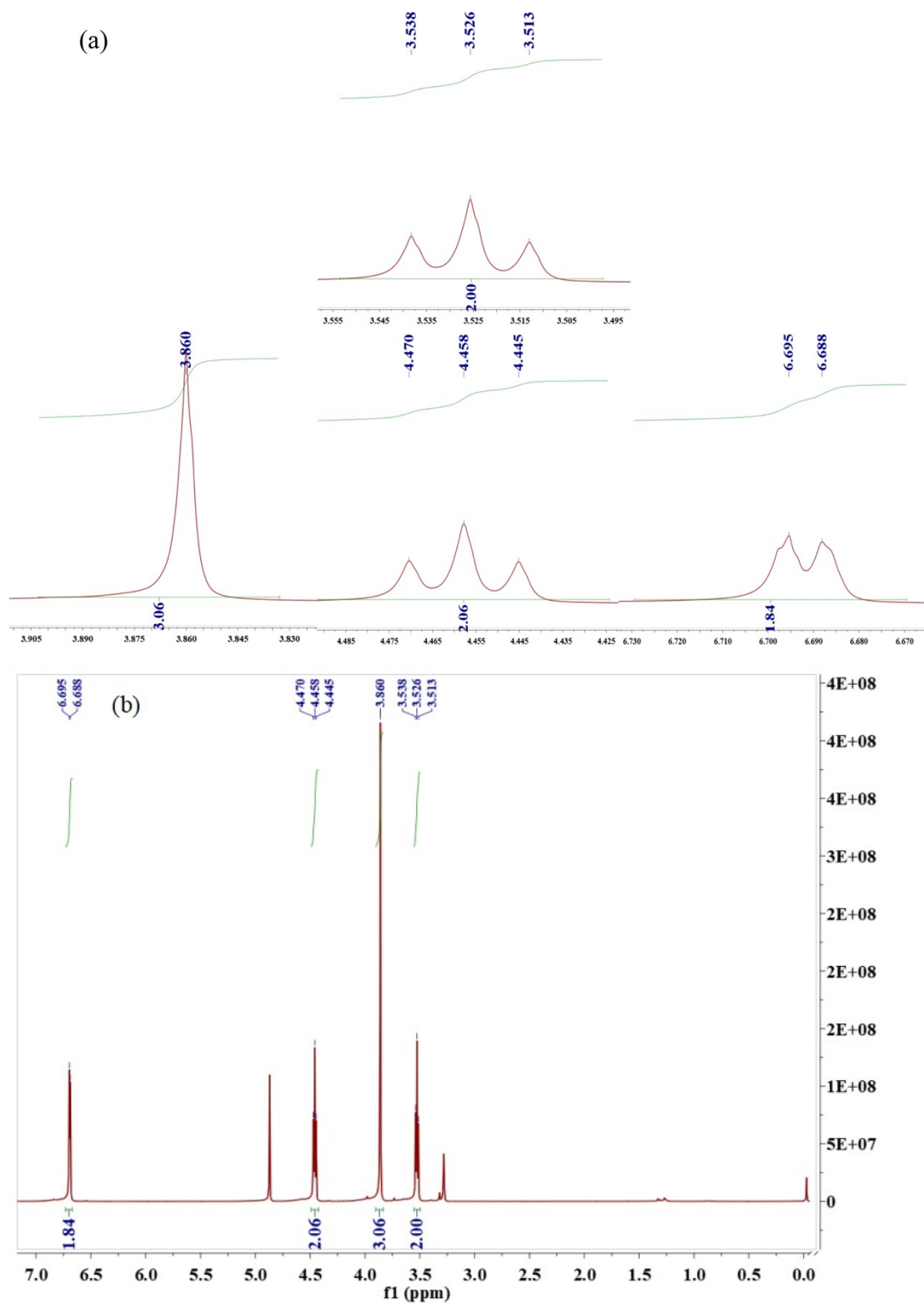


Fig. S.5. (a) the amplified spectrum of each peak at the $^1\text{H-NMR}$ spectrum. (b) $^1\text{H-NMR}$ spectrum of 5-oxo-2,3-dihydrothiazolo[3,2-a]pyridine-7-carboxylate (A-B) dissolved in CD_3OD .

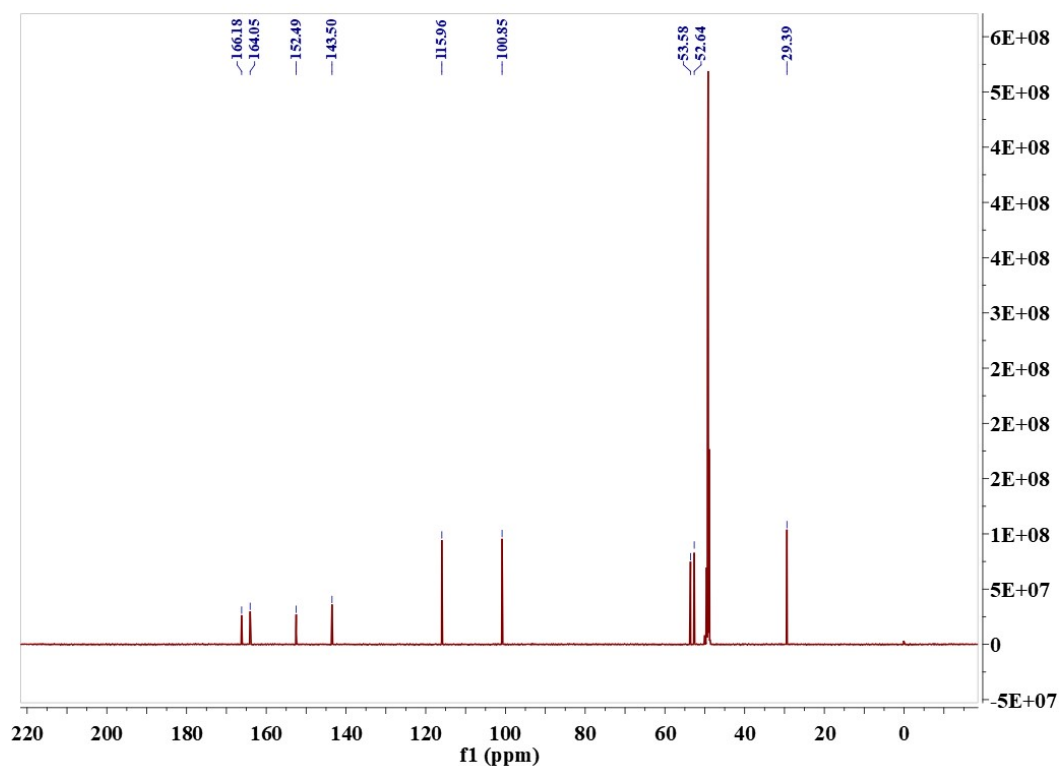


Fig. S.6. ^{13}C -NMR spectrum of 5-oxo-2,3-dihydrothiazolo[3,2-a]pyridine-7-carboxylate (A-B) dissolved in CD_3OD .

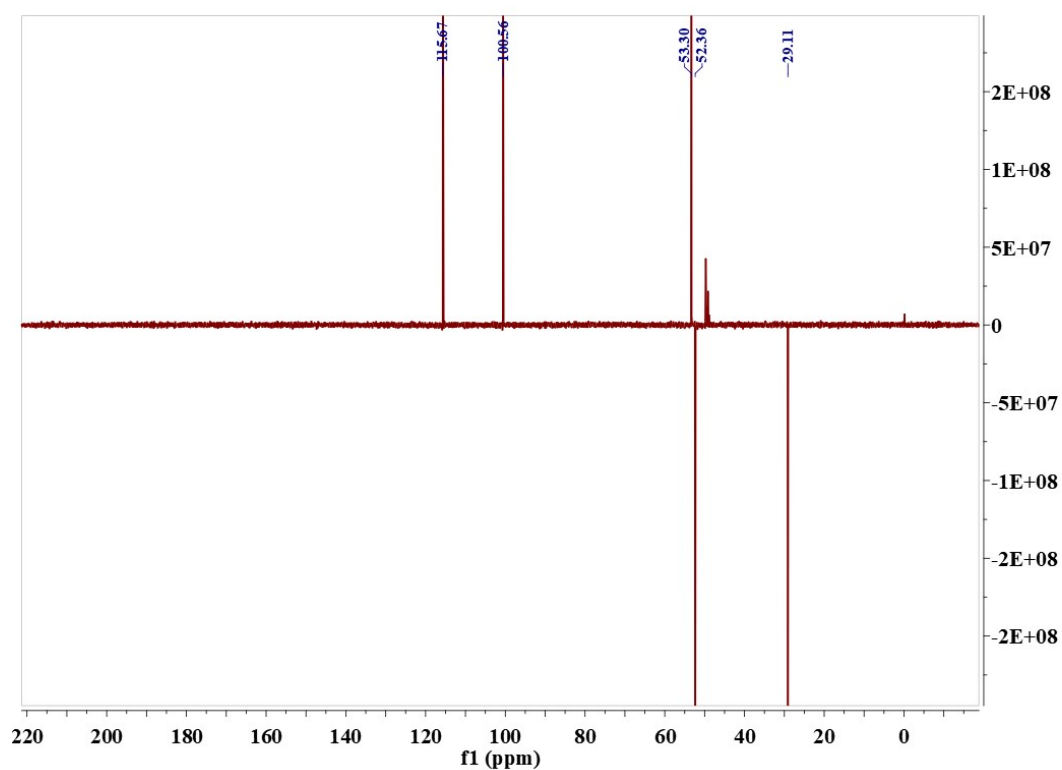


Fig. S.7. DEPT ^{13}C -NMR spectrum of 5-oxo-2,3-dihydrothiazolo[3,2-a]pyridine-7-carboxylate (A-B) dissolved in CD_3OD .

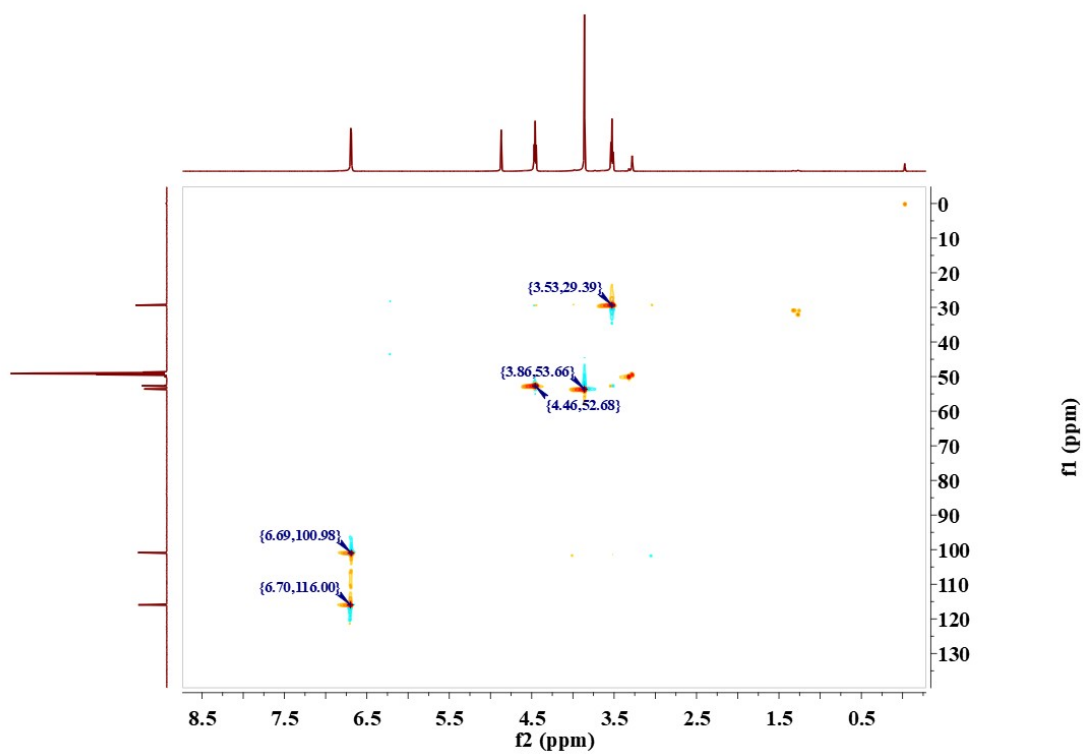


Fig. S.8. HSQC-NMR spectrum of 5-oxo-2,3-dihydrothiazolo[3,2-a]pyridine-7-carboxylate (A-B) dissolved in CD₃OD.

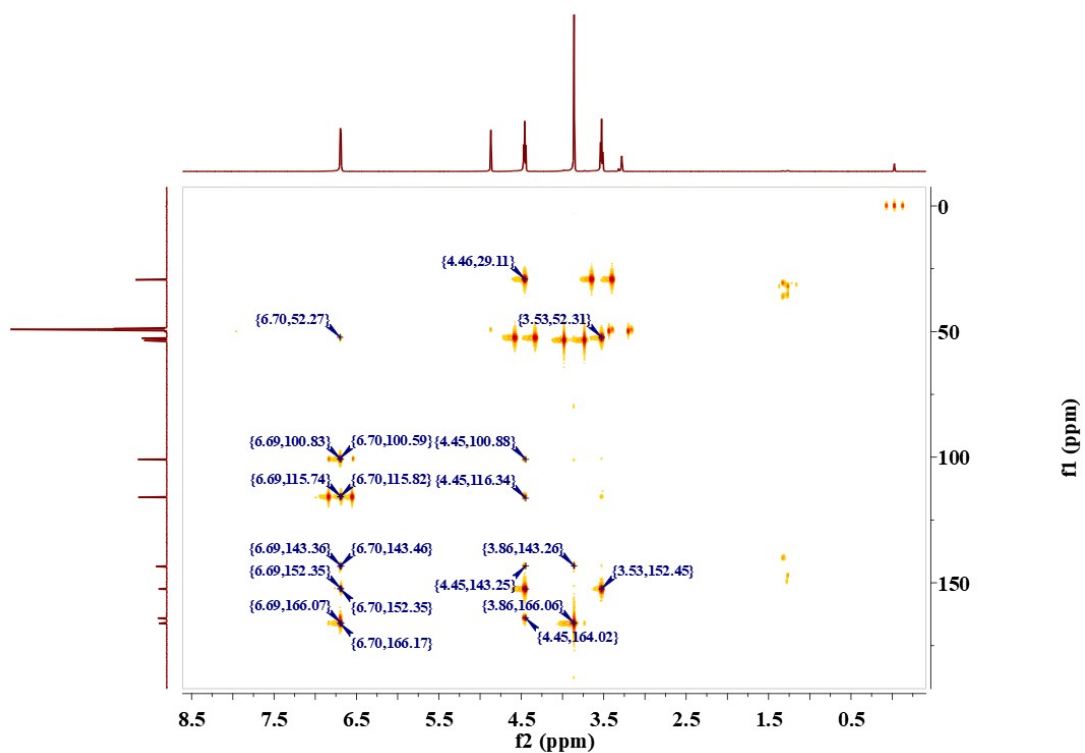


Fig. S.9. HMBC-NMR spectrum of 5-oxo-2,3-dihydrothiazolo[3,2-a]pyridine-7-carboxylate (A-B) dissolved in CD₃OD.

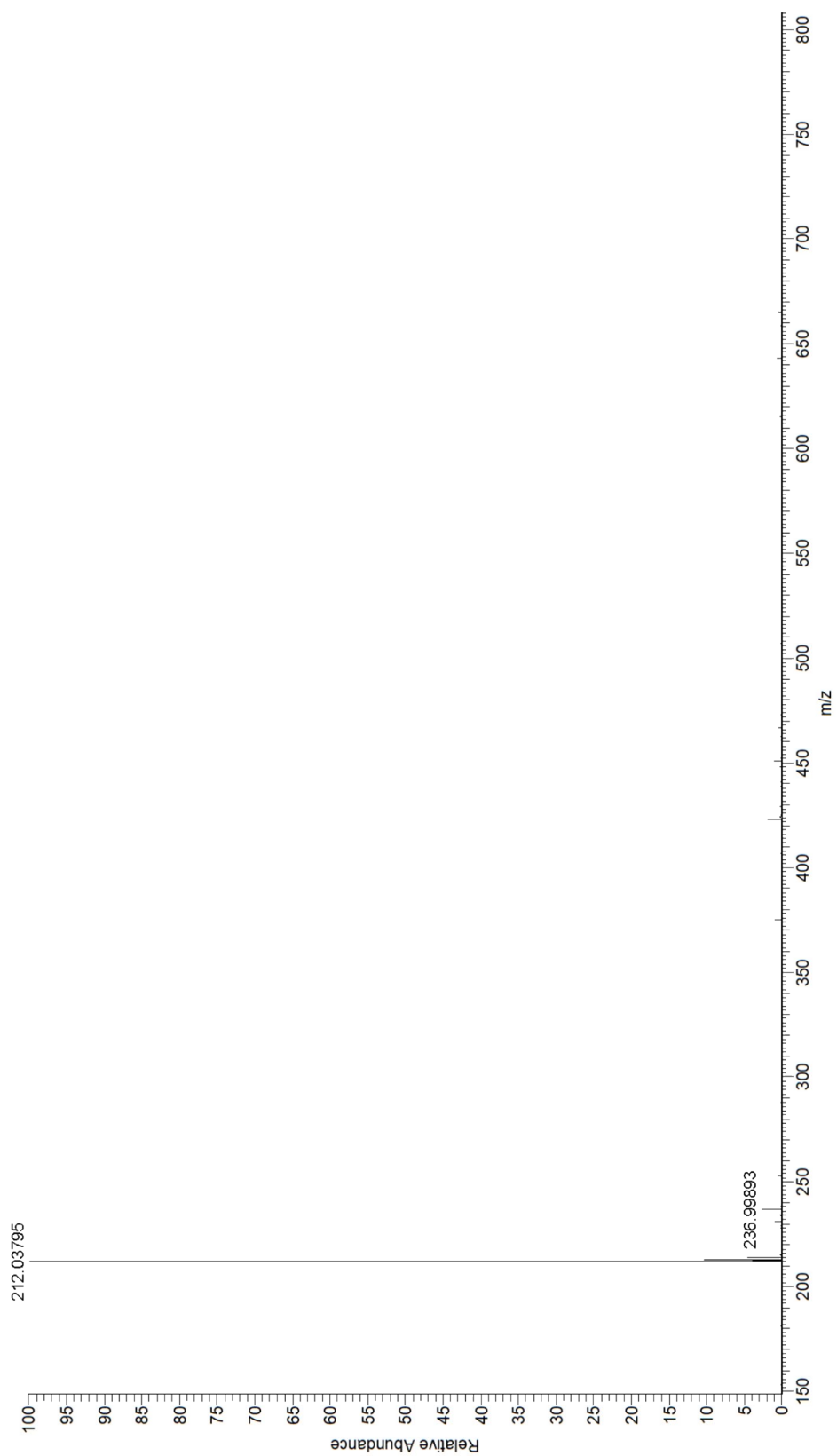


Fig. S.10. ESI-HRMS mass spectrum of methyl 5-oxo-2,3-dihydrothiazolo[3,2-a] pyridine-7-Carboxylate (A-B).

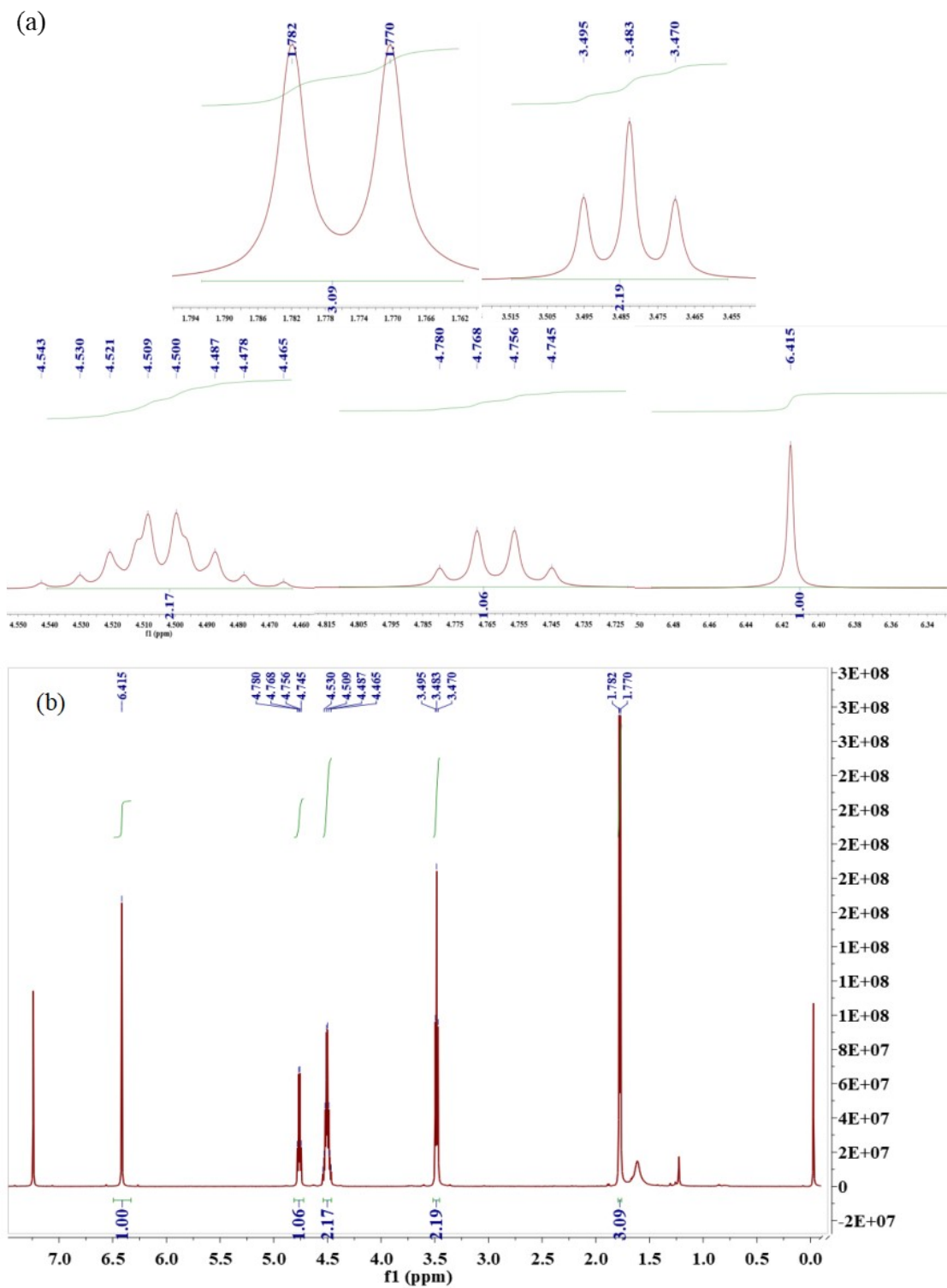


Fig. S.11. (a) is the amplified spectrum of each peak at the $^1\text{H-NMR}$ spectrum. (b) is $^1\text{H-NMR}$ spectrum of 2,3-dihydrothiazolo[3,2-a]thiopyrano[3,4-d]pyridine-5,10-dione (A-G) dissolved in CD_3CL .

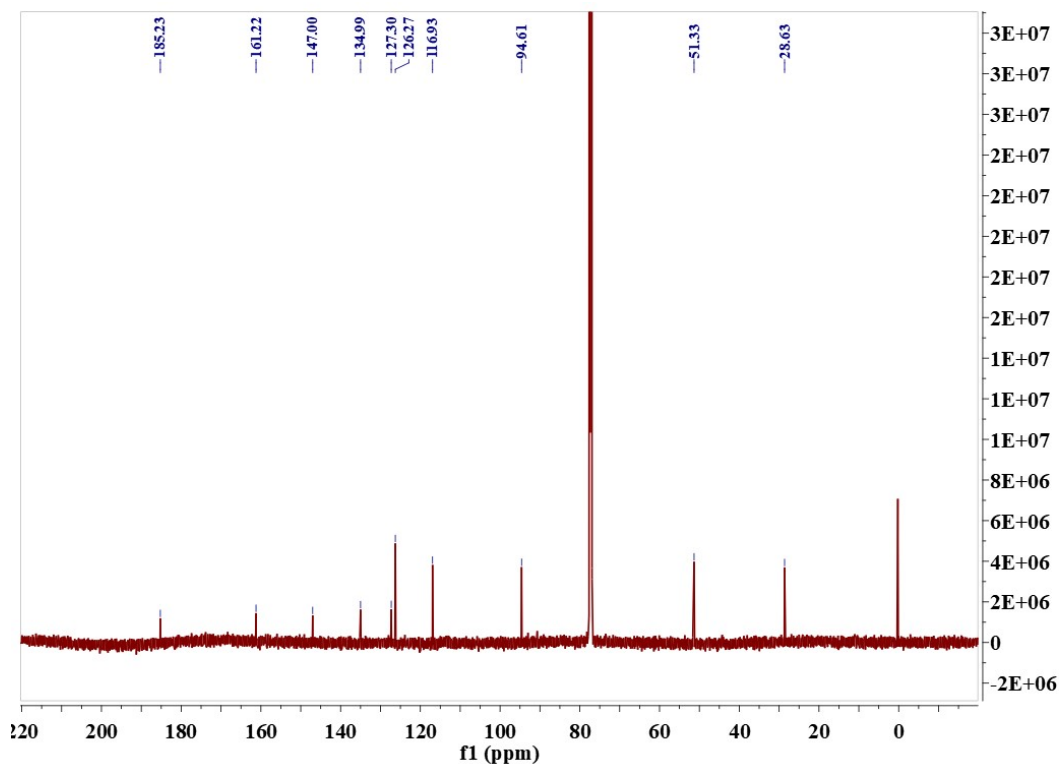


Fig. S.12. ^{13}C -NMR spectrum of 2,3-dihydrothiazolo[3,2-a]thiopyrano[3,4-d]pyridine-5,10-dione (A-G) dissolved in CD_3CL .

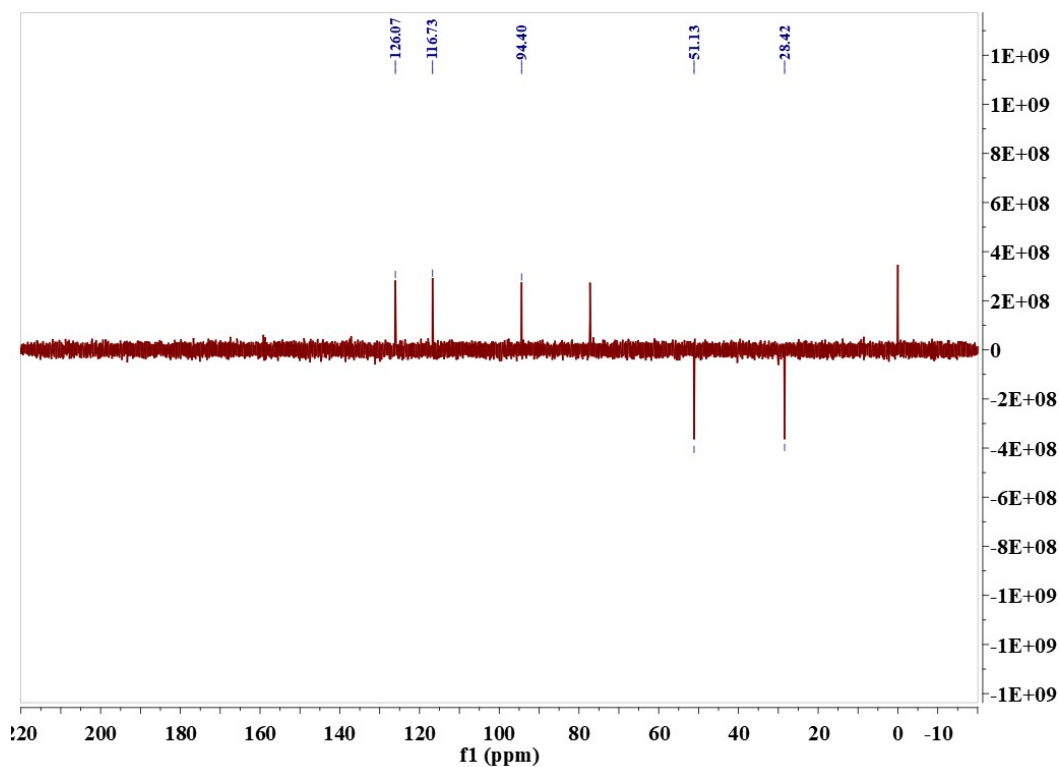


Fig. S.13. Dept 135-NMR spectrum of 2,3-dihydrothiazolo[3,2-a]thiopyrano[3,4-d]pyridine-5,10-dione (A-G) dissolved in CD_3CL .

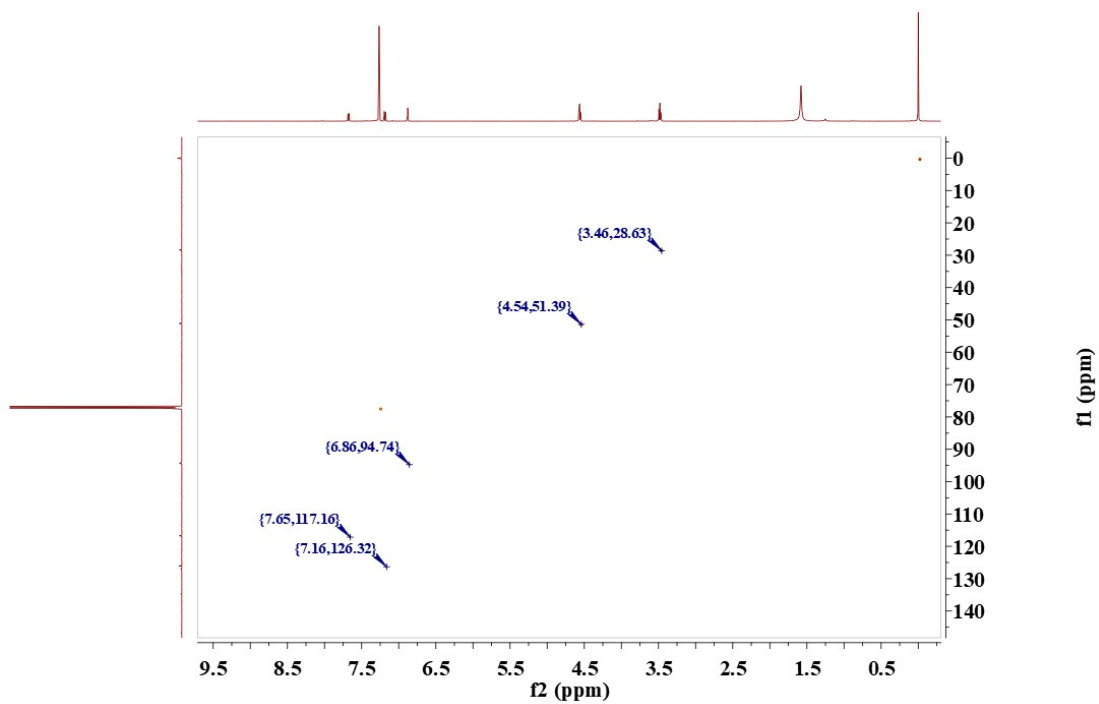


Fig. S.14. HSQC-NMR spectrum of 2,3-dihydrothiazolo[3,2-a]thiopyrano[3,4-d] pyridine -5,10-dione (A-G) dissolved in CD₃CL.

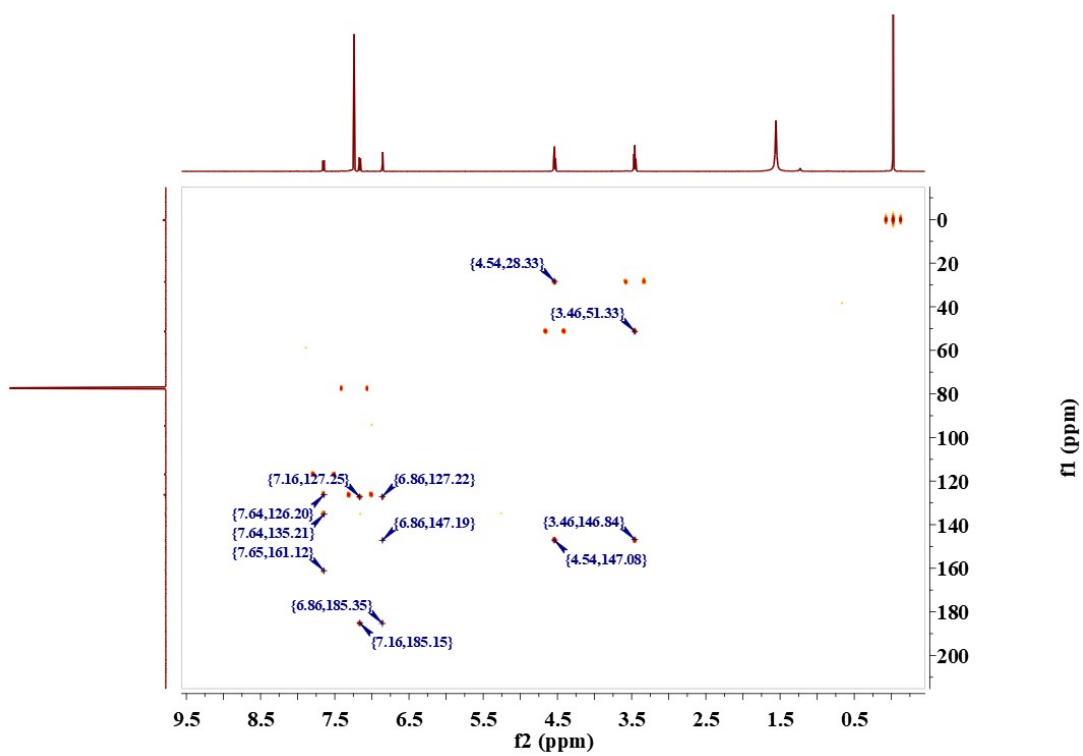


Fig. S.15. HMBC-NMR spectrum of 2,3-dihydrothiazolo[3,2-a]thiopyrano[3,4-d] pyridine -5,10-dione (A-G) dissolved in CD₃CL.

LI-AG_190404153213 #1673 RT: 23.37 AV: 1 NL: 6.36E7
T: FTMS + p ESI Full lock ms [150.0000-1100.0000]

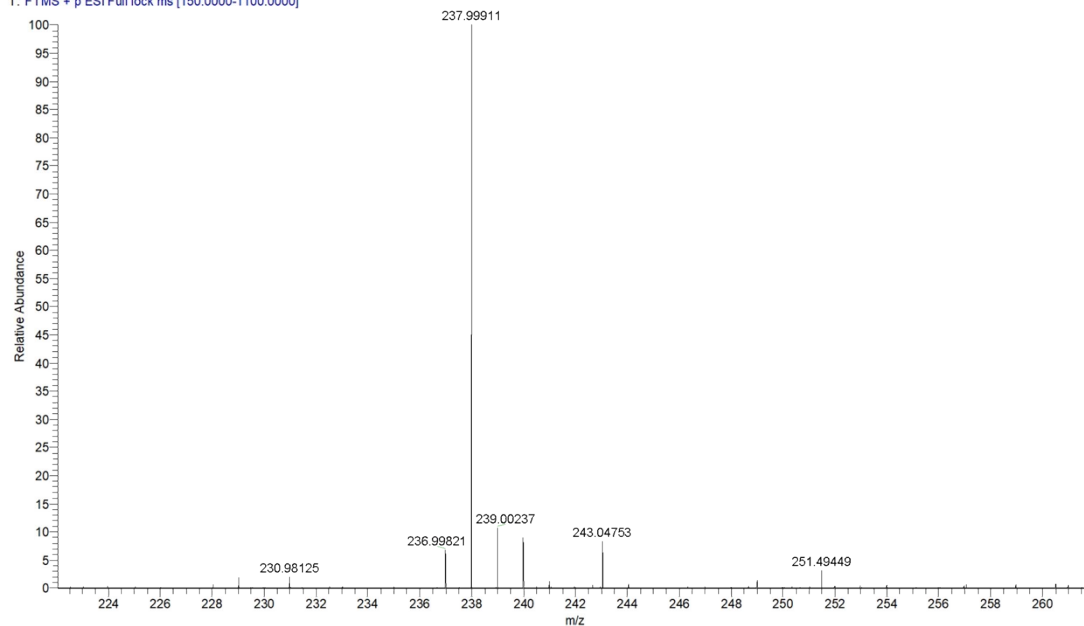
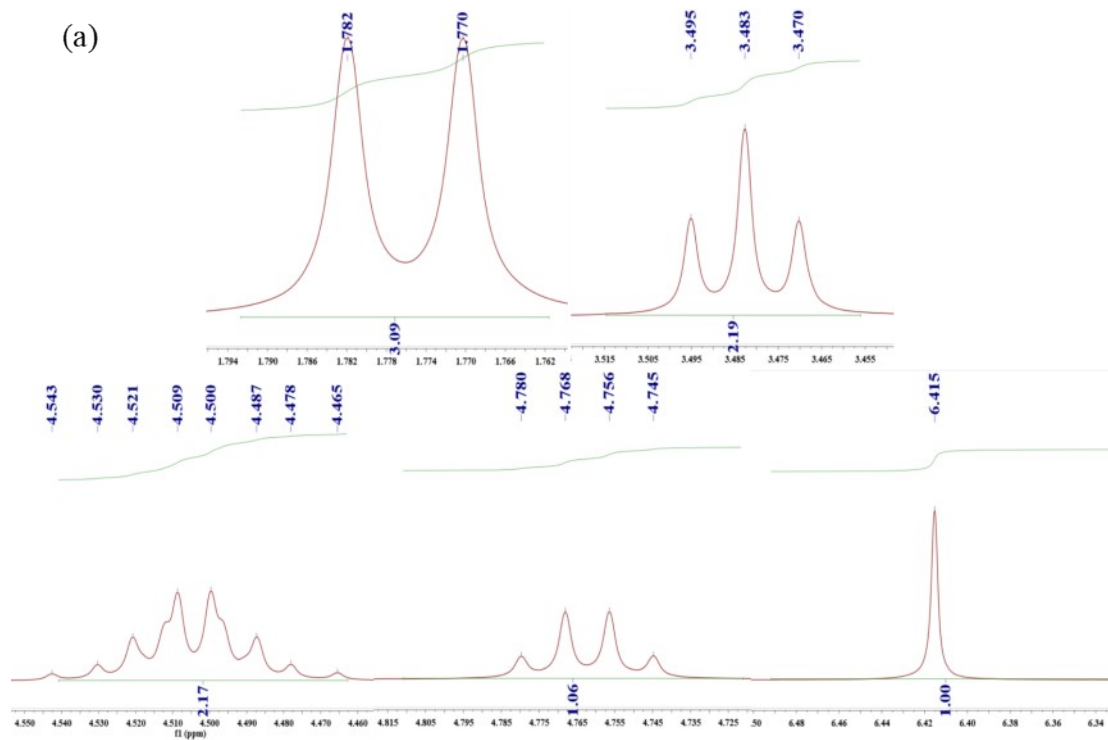


Fig. S.16. ESI-HRMS mass spectrum of 2,3-dihydrothiazolo[3,2-a]thiopyrano[3,4-d]pyridine - 5,10-dione (A-G).



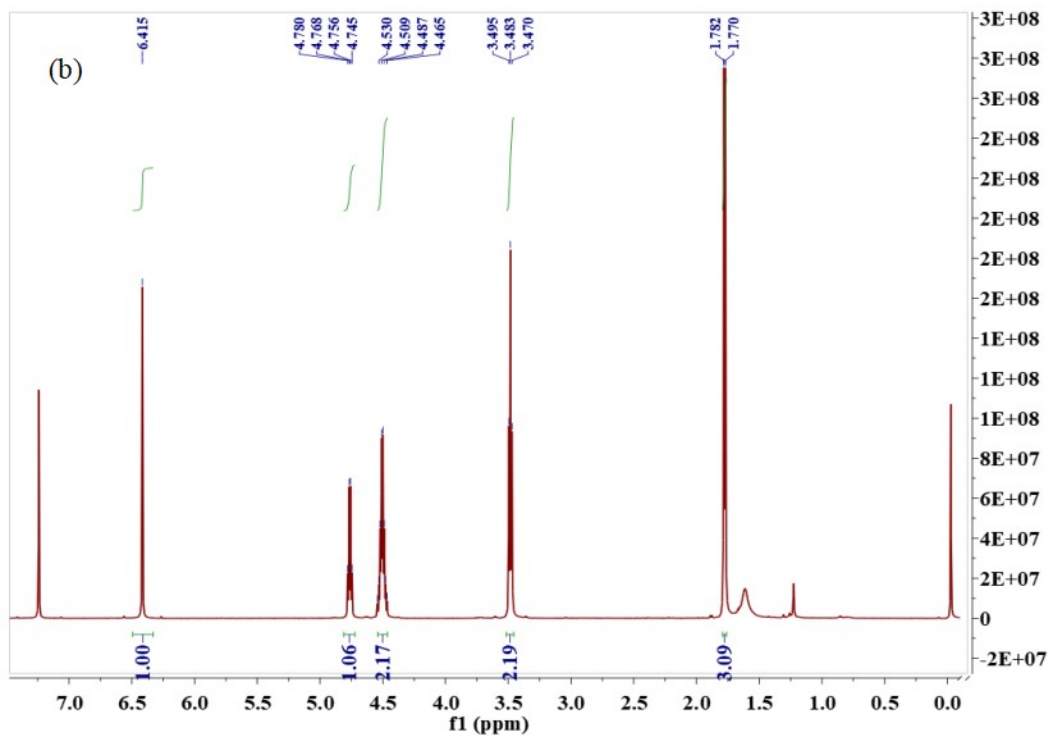


Fig. S.17. (a) is the amplified spectrum of each peak at the ^1H -NMR spectrum. (b) is ^1H -NMR spectrum of 7-methyl-2,3-dihydrothiazolo[3,2-a]-7H-thieno[3,4-d]pyridine-5,9-dione (A-BG) dissolved in CD_3CL .

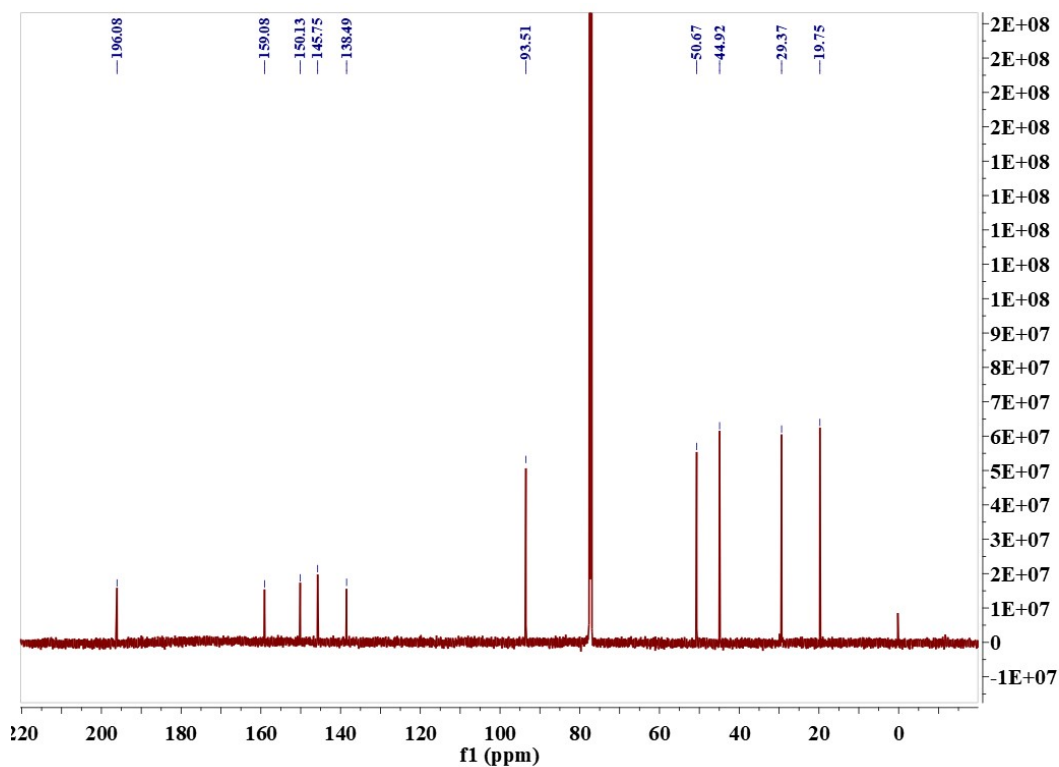


Fig. S.18. ^{13}C -NMR spectrum of 7-methyl-2,3-dihydrothiazolo[3,2-a]-7H-thieno[3,4-d]pyridine-5,9-dione (A-BG) dissolved in CD_3CL .

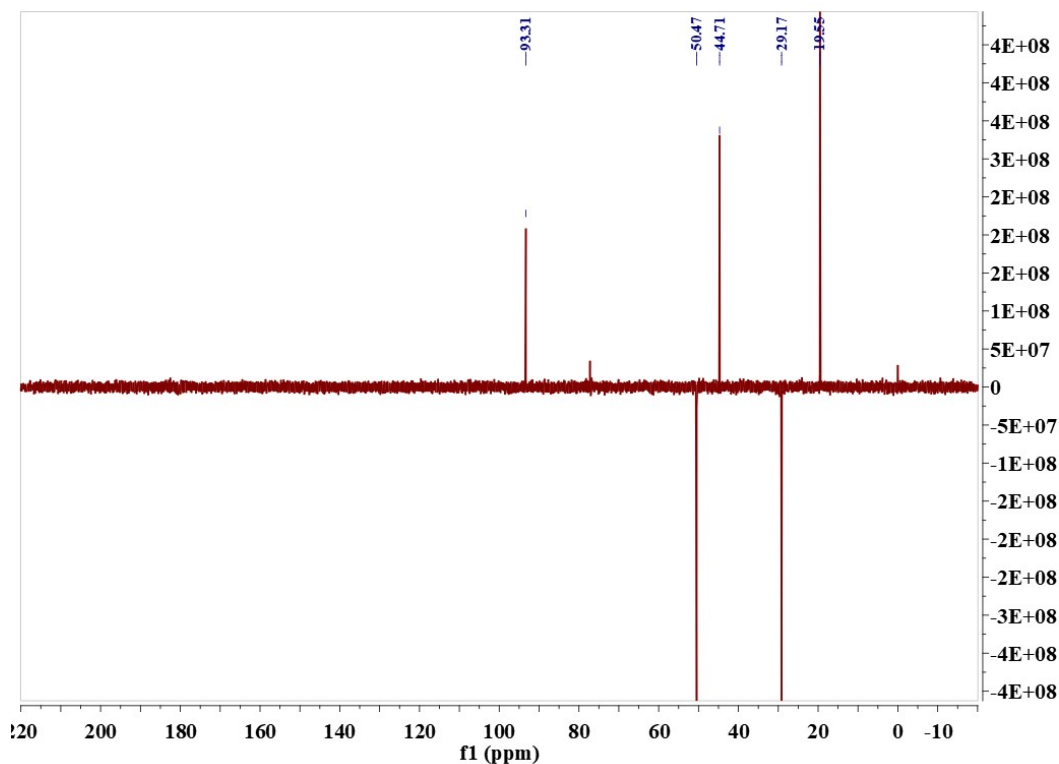


Fig. S.19. Dept 135-NMR spectrum of 7-methyl-2,3-dihydrothiazolo[3,2-a]-7H-thieno[3,4-d]pyridine -5,9-dione (A-BG) dissolved in CD₃CL.

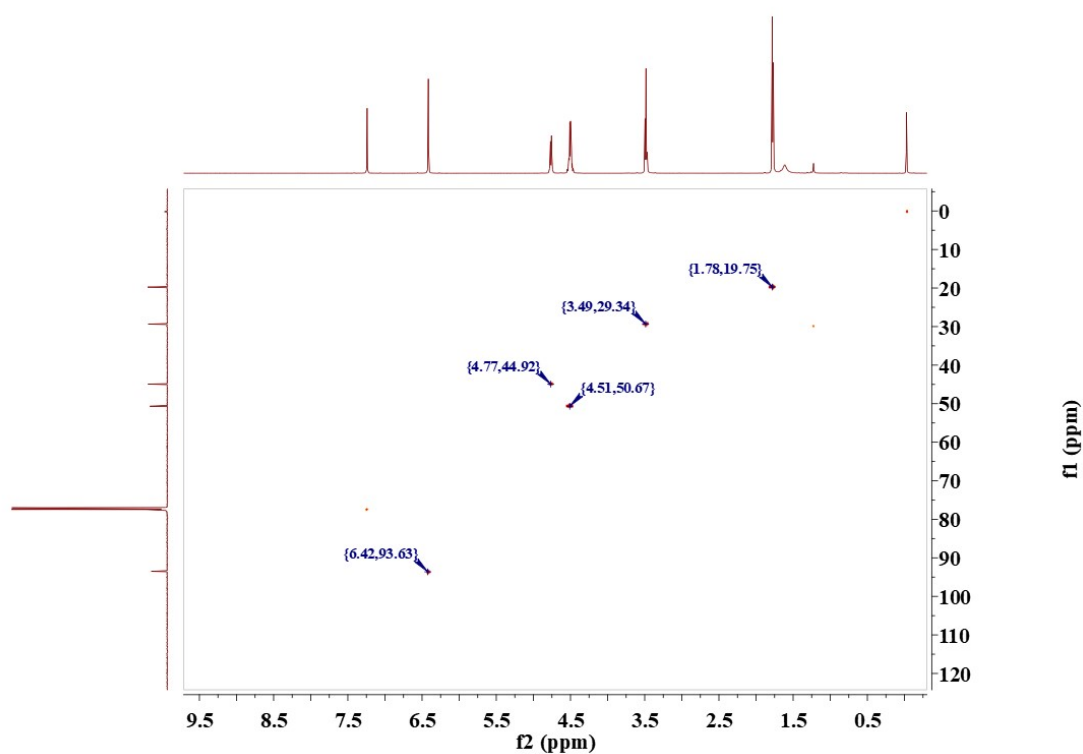


Fig. S.20. HSQC-NMR spectrum of 7-methyl-2,3-dihydrothiazolo[3,2-a]-7H-thieno[3,4-d]pyridine-5,9-dione (A-BG) dissolved in CD₃CL.

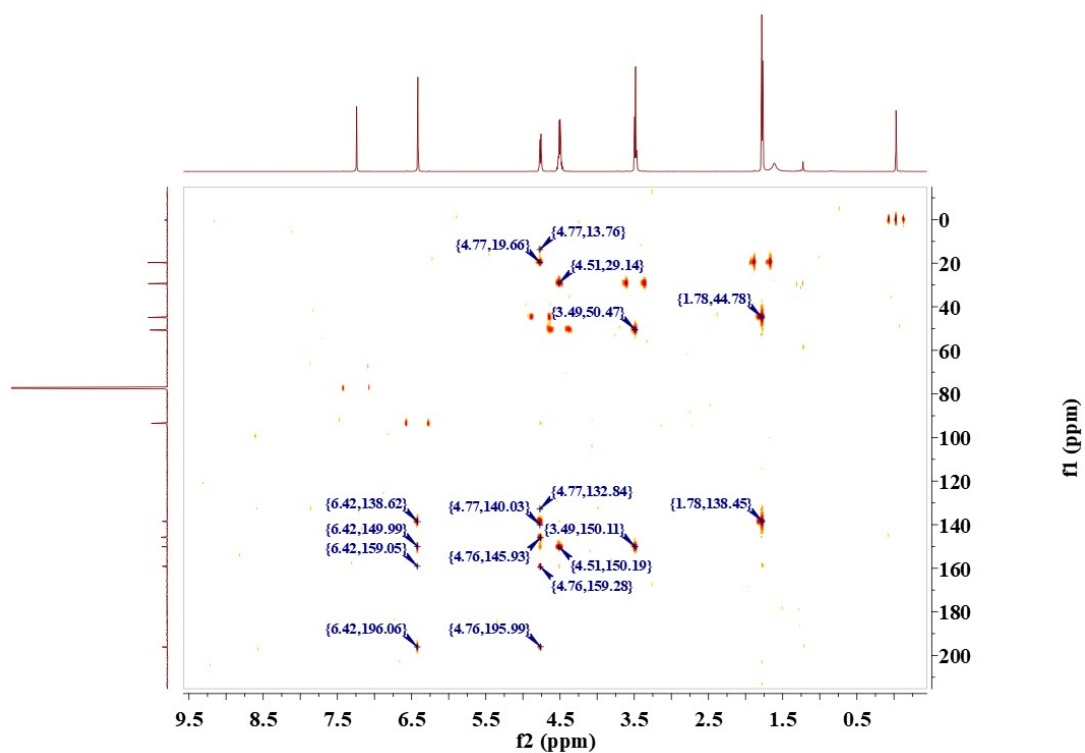


Fig. S.21. HMBC-NMR spectrum of 7-methyl-2,3-dihydrothiazolo[3,2-a]-7H-thieno[3,4-d]pyridine-5,9-dione (A-BG) dissolved in CD₃CL.

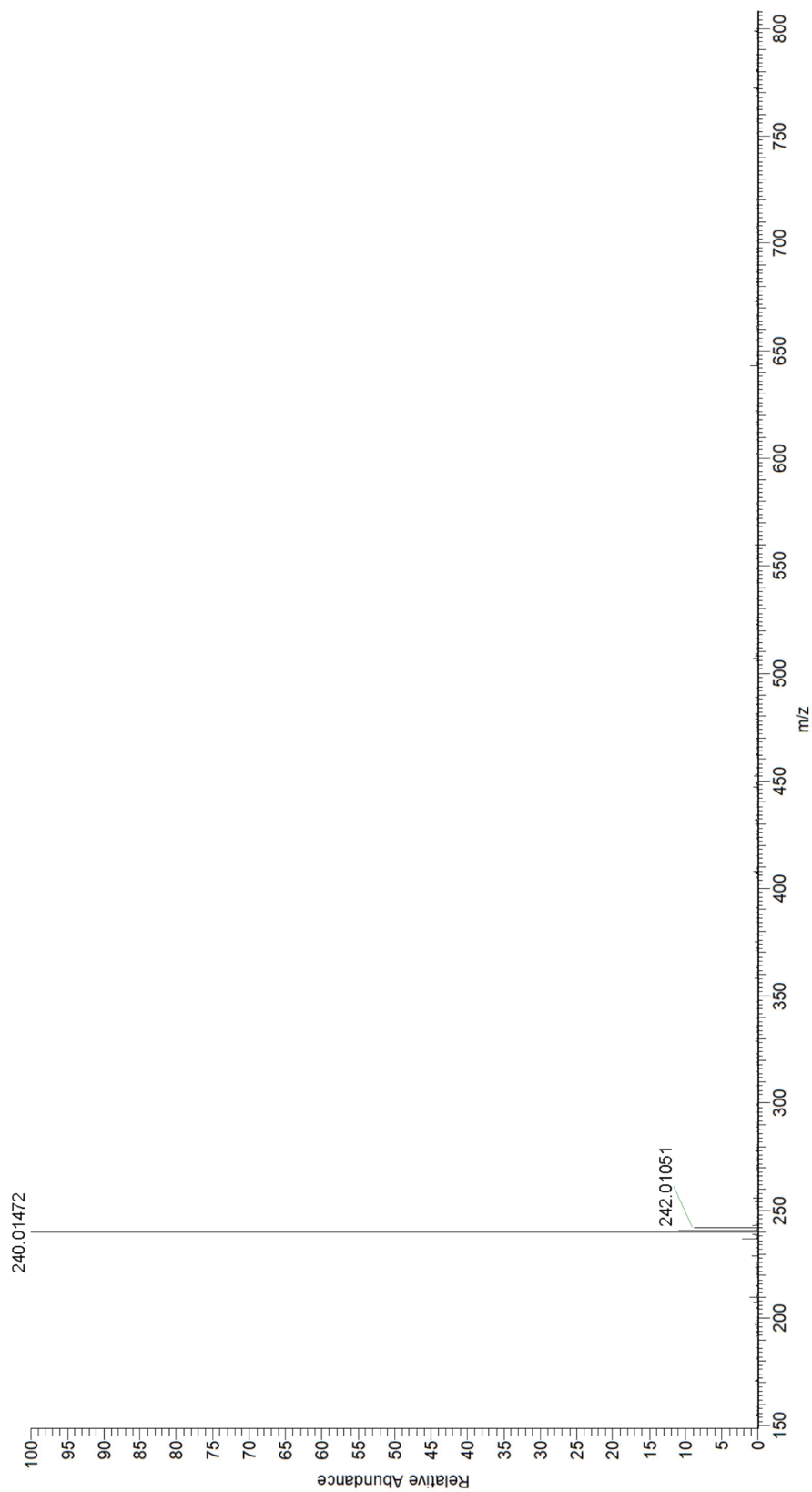


Fig. S.22. ESI-HRMS mass spectrum of 7-methyl-2,3-dihydrothiazolo[3,2-a]-7H-thieno[3,4-d]pyridine-5,9-dione (A-BG).

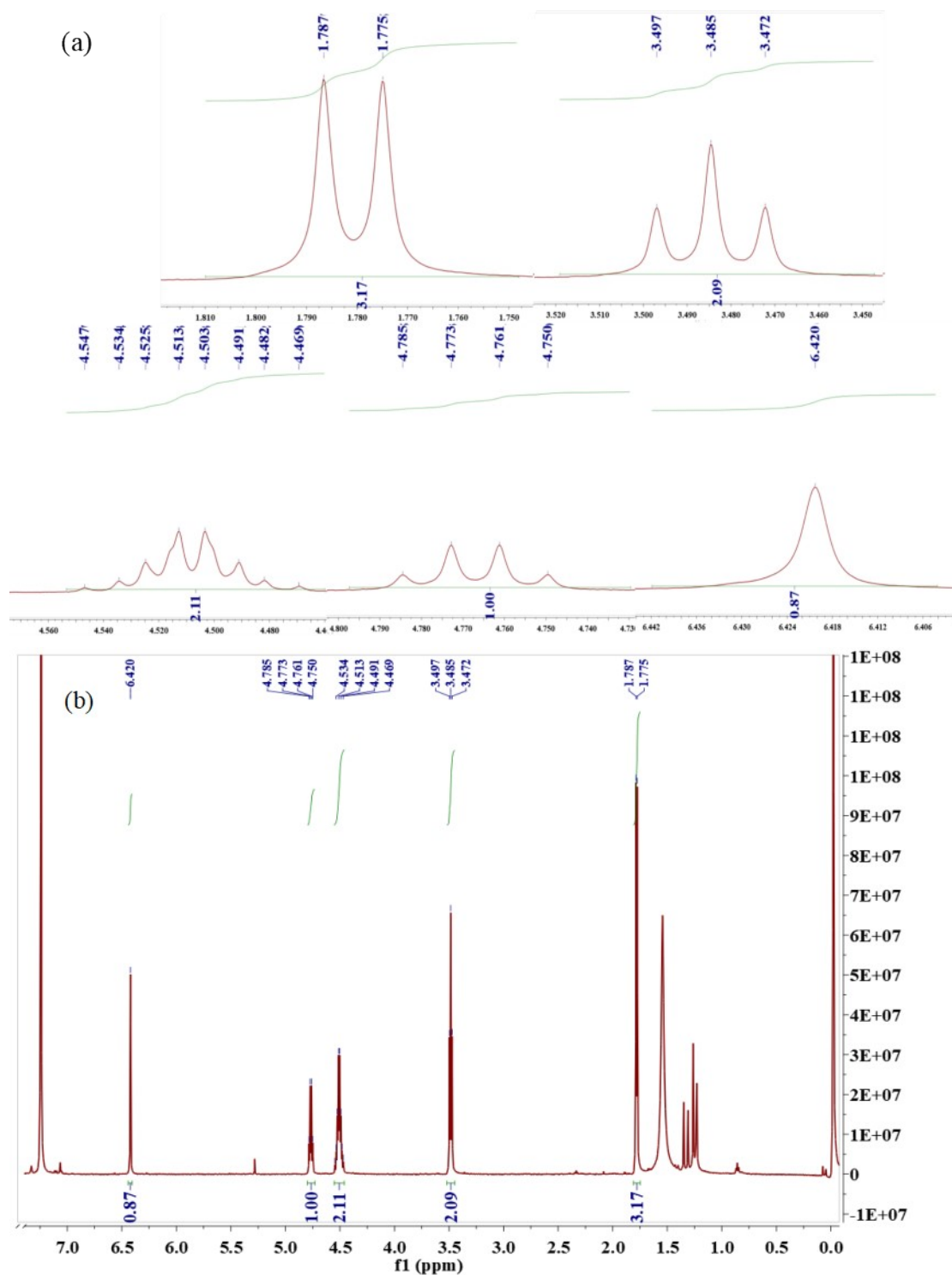


Fig. S.23. (a) is the amplified spectrum of each peak at the $^1\text{H-NMR}$ spectrum. (b) is $^1\text{H-NMR}$ spectrum of 7-methyl-2,3-dihydrothiazolo[3,2-a]-7H-thieno[3,4-d]pyridine-5,9-dione (B-BG-1) dissolved in CD_3CL .

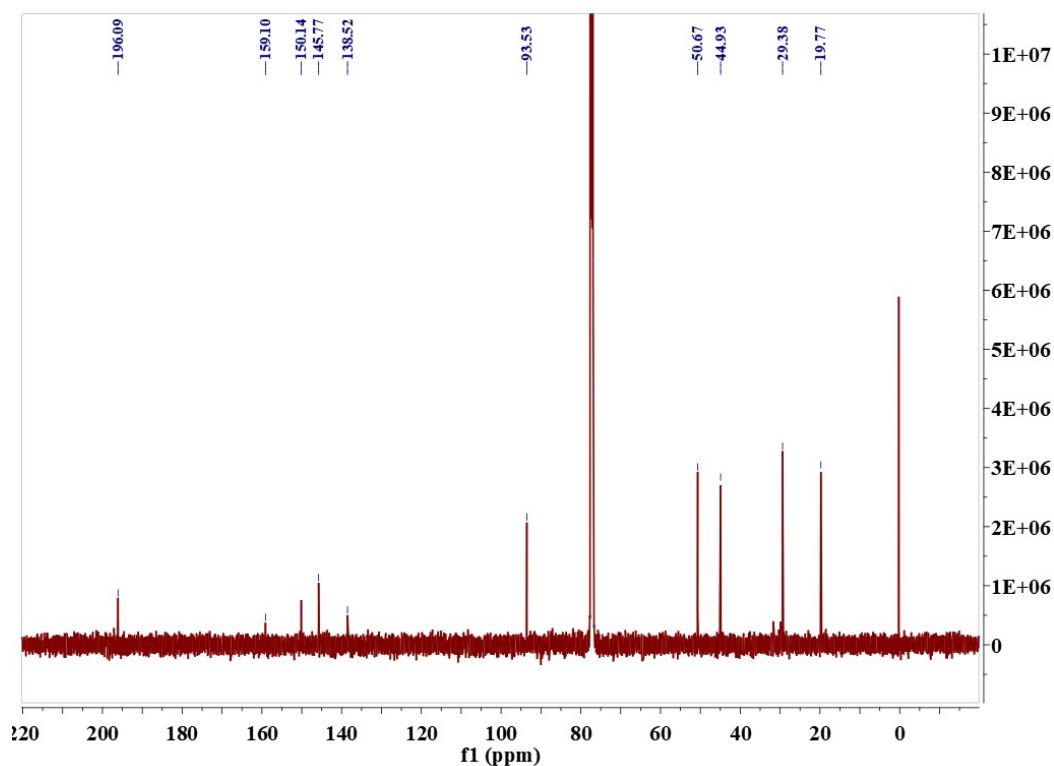


Fig. S.24. ^{13}C -NMR spectrum of 7-methyl-2,3-dihydrothiazolo[3,2-a]-7H-thieno[3,4-d]Pyridine-5,9-dione (B-BG-1) dissolved in CD_3CL .

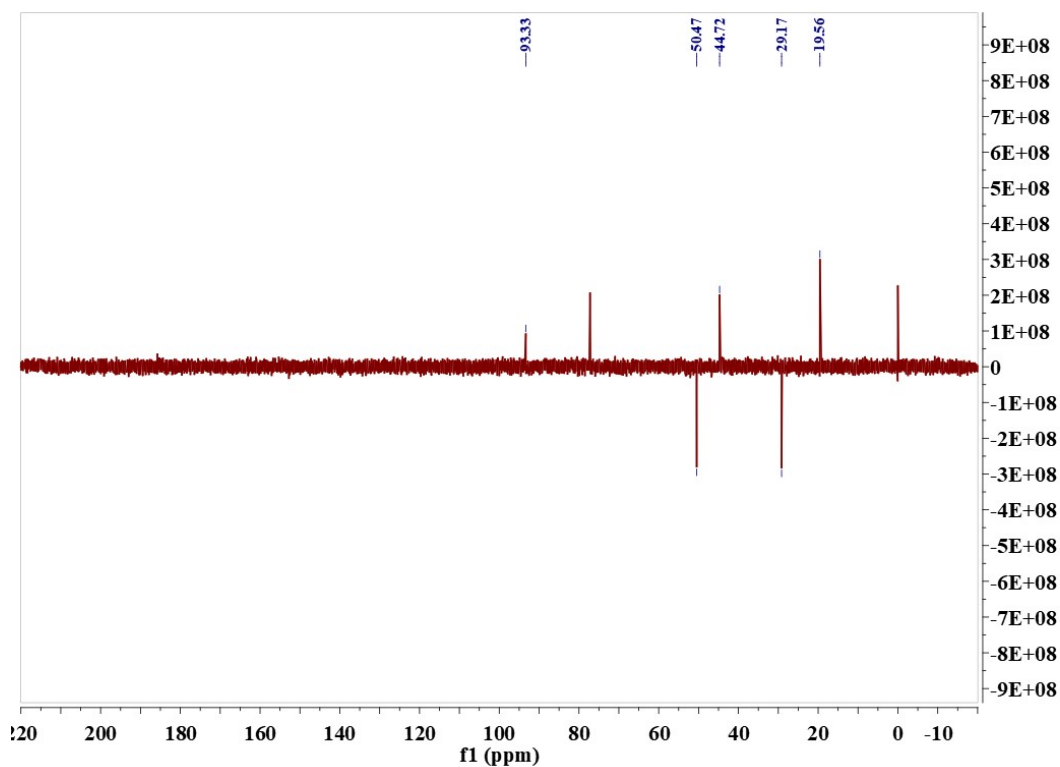


Fig. S.25. Dept ^{135}C -NMR spectrum of 7-methyl-2,3-dihydrothiazolo[3,2-a]-7H-thieno[3,4-d]pyridine -5,9-dione (B-BG-1) dissolved in CD_3CL .

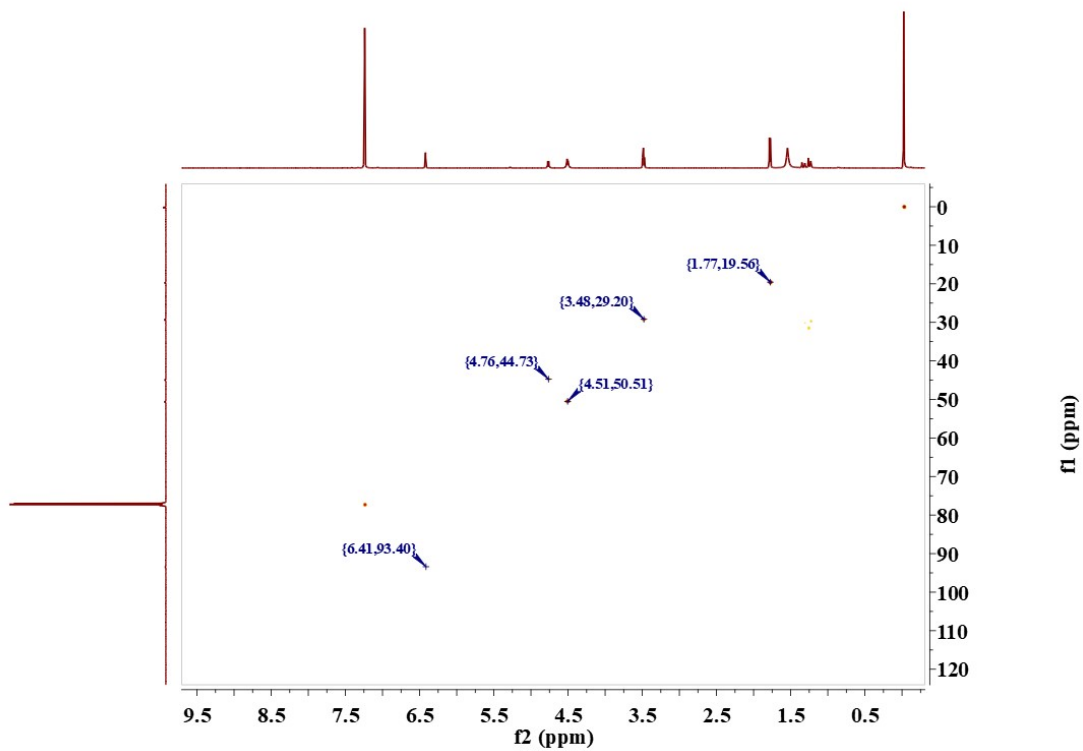


Fig. S.26. HSQC-NMR spectrum of 7-methyl-2,3-dihydrothiazolo[3,2-a]-7H-thieno[3,4-d]pyridine-5,9-dione (B-BG-1) dissolved in CD_3CL .

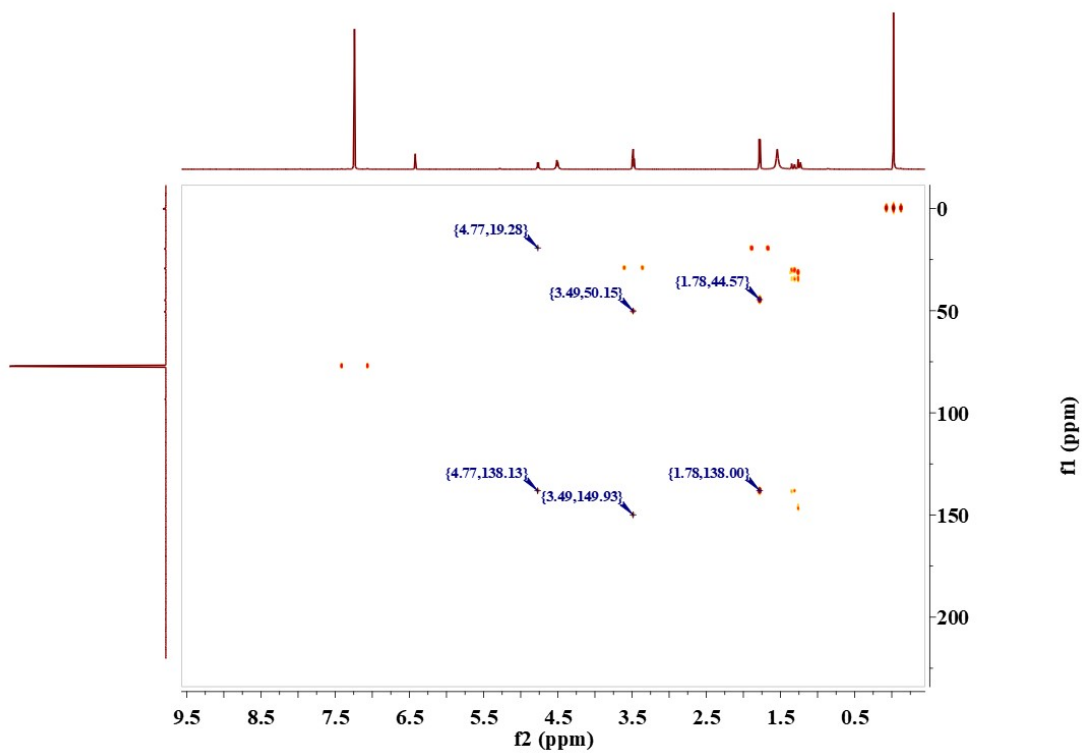


Fig. S.27. HMBC-NMR spectrum of 7-methyl-2,3-dihydrothiazolo[3,2-a]-7H-thieno[3,4-d]pyridine-5,9-dione (B-BG-1) dissolved in CD_3CL .

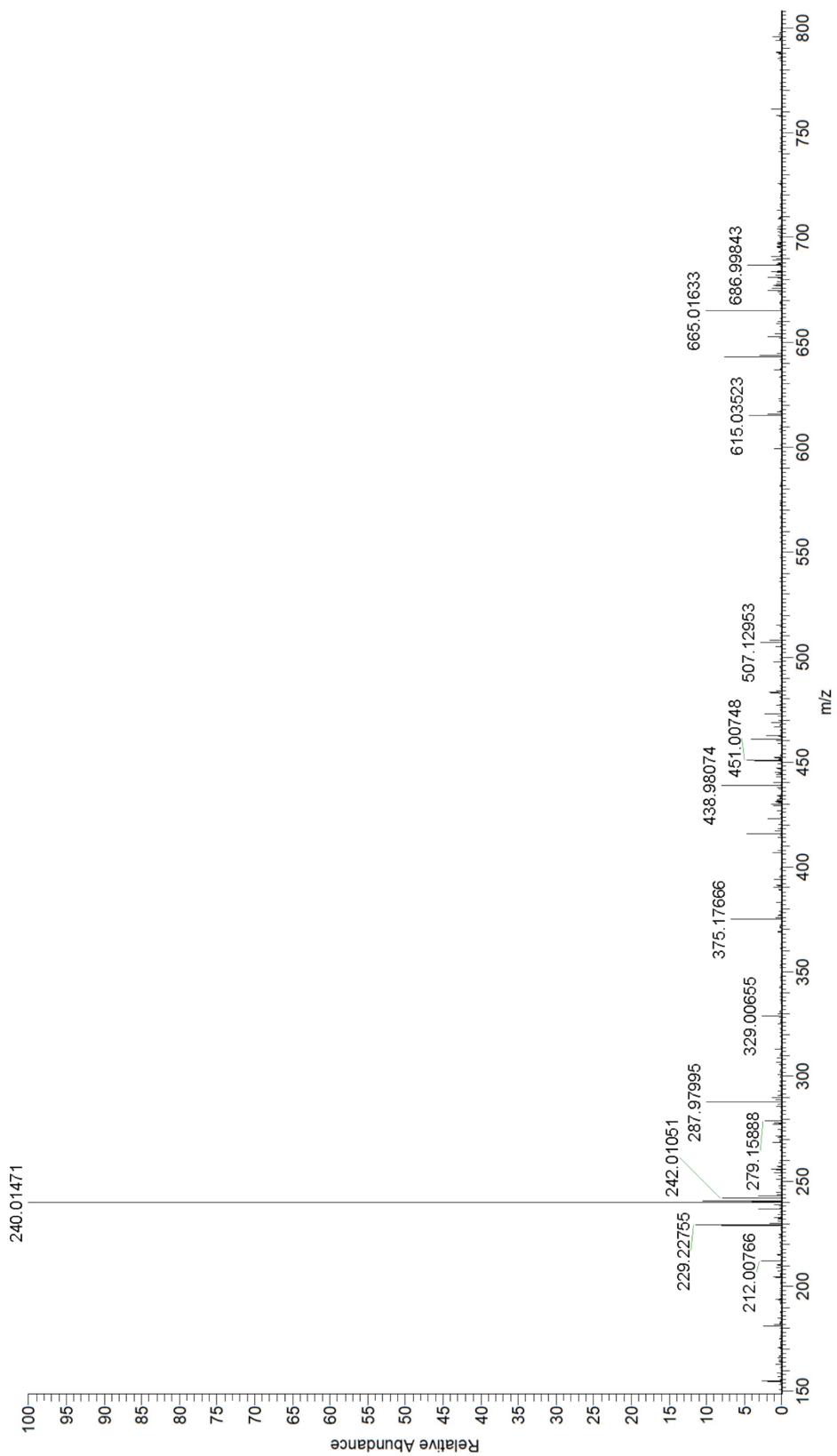


Fig. S.28. ESI-HRMS mass spectrum of 7-methyl-2,3-dihydrothiazolo[3,2-a]-7H-thieno[3,4-d]pyridine-5,9-dione (B-BG-1) dissolved.

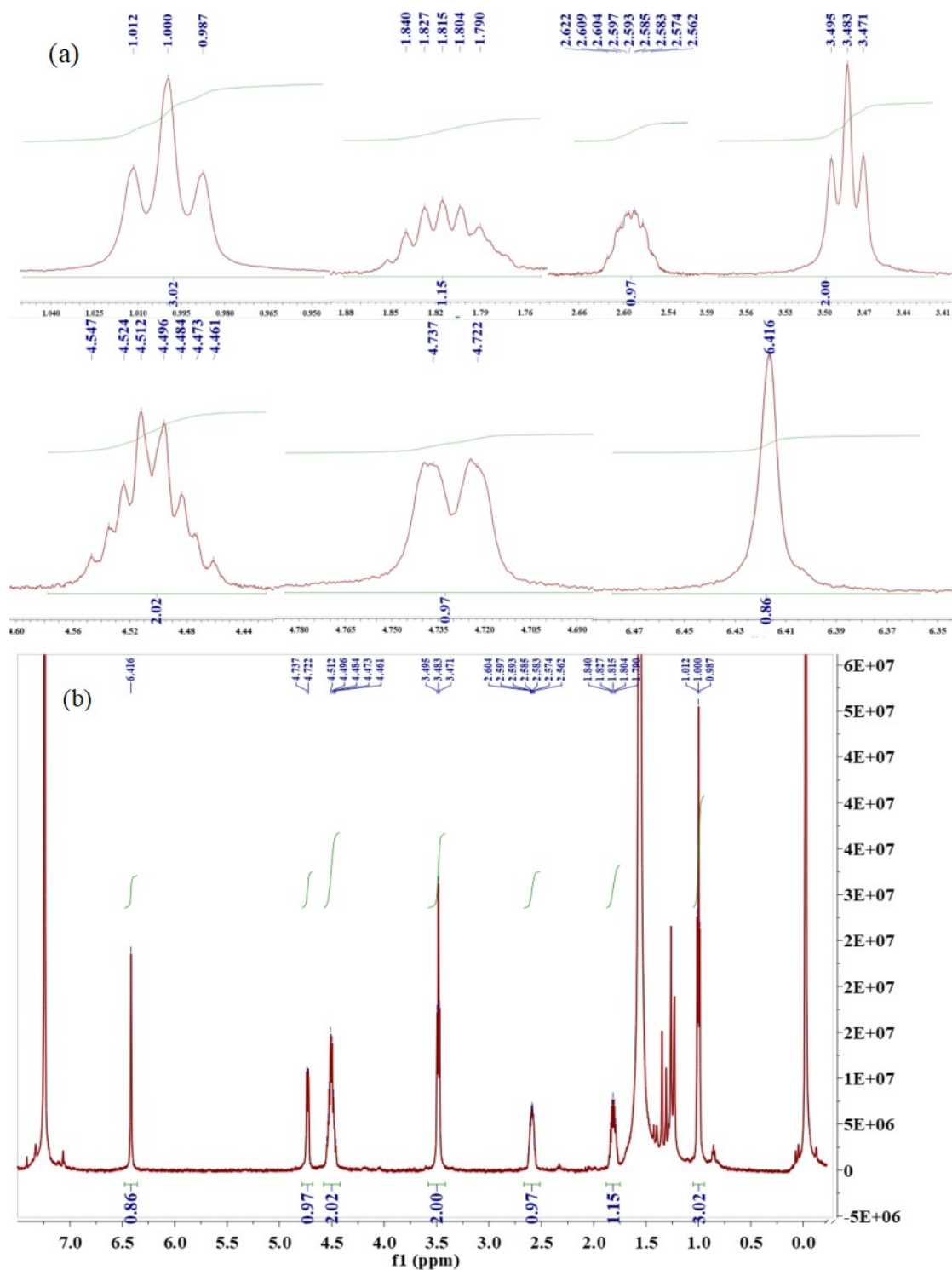


Fig. S.29. (a) is the amplified spectrum of each peak at the $^1\text{H-NMR}$ spectrum. (b) is $^1\text{H-NMR}$ spectrum of 7-ethyl-2,3-dihydrothiazolo[3,2-a]-7H-thieno[3,4-d]pyridine-5,9-dione (B-G-2) dissolved in CD_3CL .

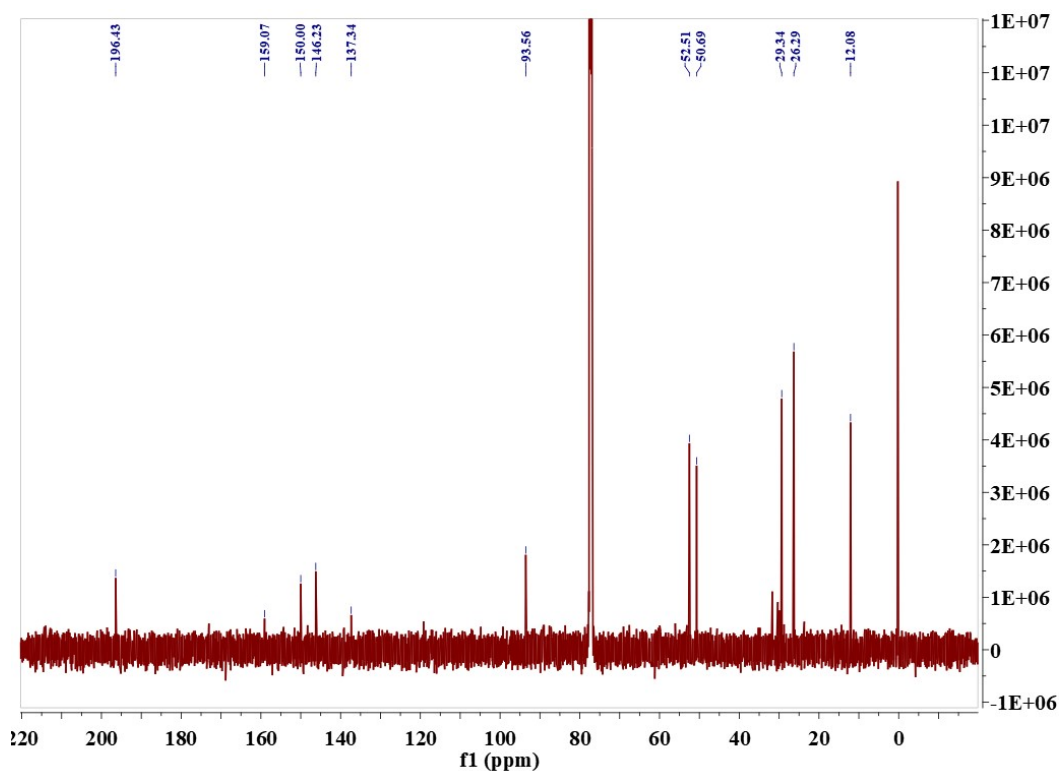


Fig. S.30. ^{13}C -NMR spectrum of 7-ethyl-2,3-dihydrothiazolo[3,2-a]-7H-thieno[3,4-d]pyridine-5,9-dione (B-G-2) dissolved in CD_3CL .

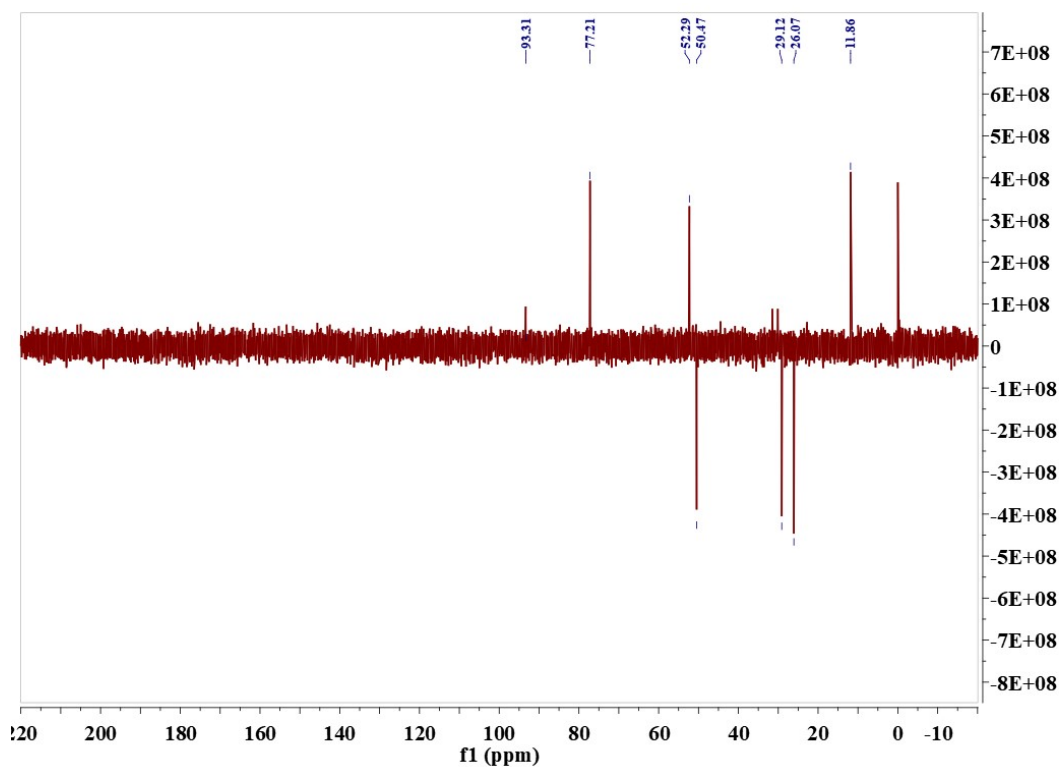


Fig. S.31. Dept 135-NMR spectrum of 7-ethyl-2,3-dihydrothiazolo[3,2-a]-7H-thieno[3,4-d]pyridine-5,9-dione (B-G-2) dissolved in CD_3CL .

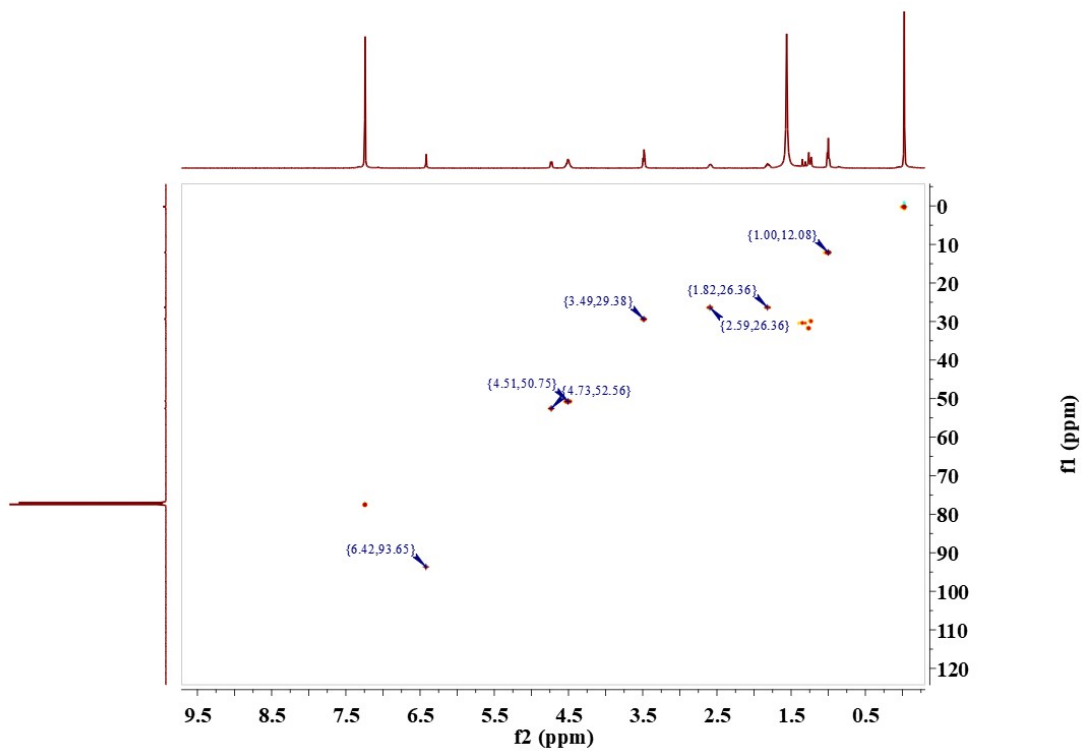


Fig. S.32. HSQC-NMR spectrum of 7-ethyl-2,3-dihydrothiazolo[3,2-a]-7H-thieno[3,4-d] pyridine-5,9-dione (B-G-2) dissolved in CD₃CL.

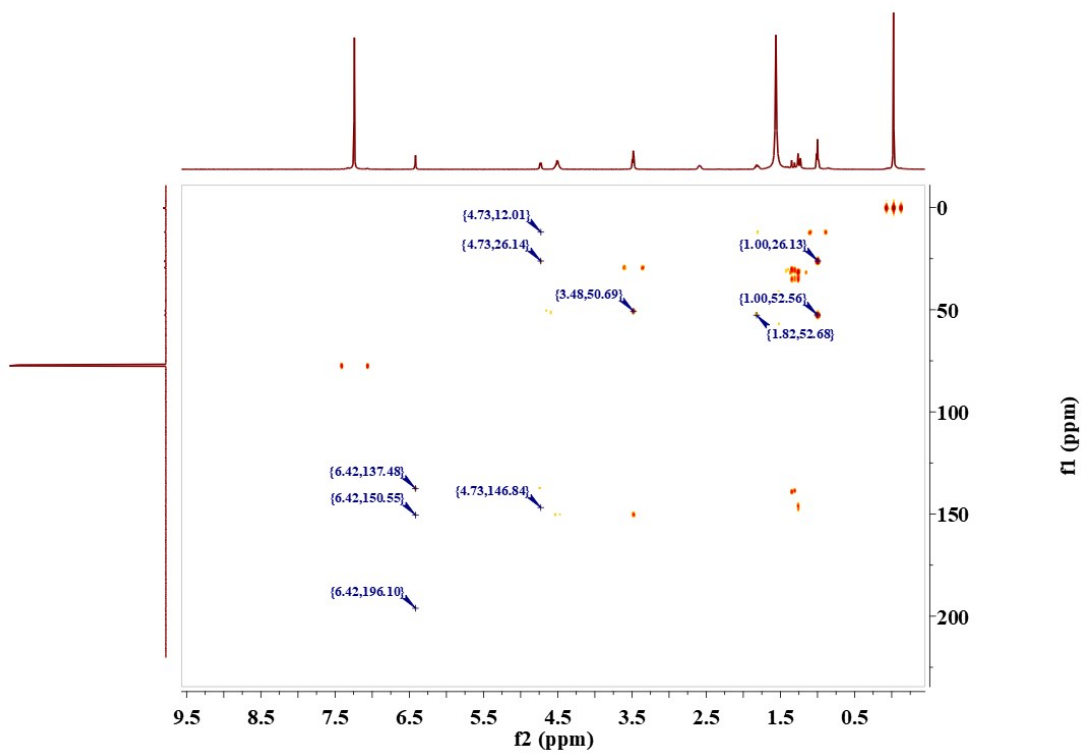


Fig. S.33. HMBC-NMR spectrum of 7-ethyl-2,3-dihydrothiazolo[3,2-a]-7H-thieno[3,4-d] pyridine-5,9-dione (B-G-2) dissolved in CD₃CL.

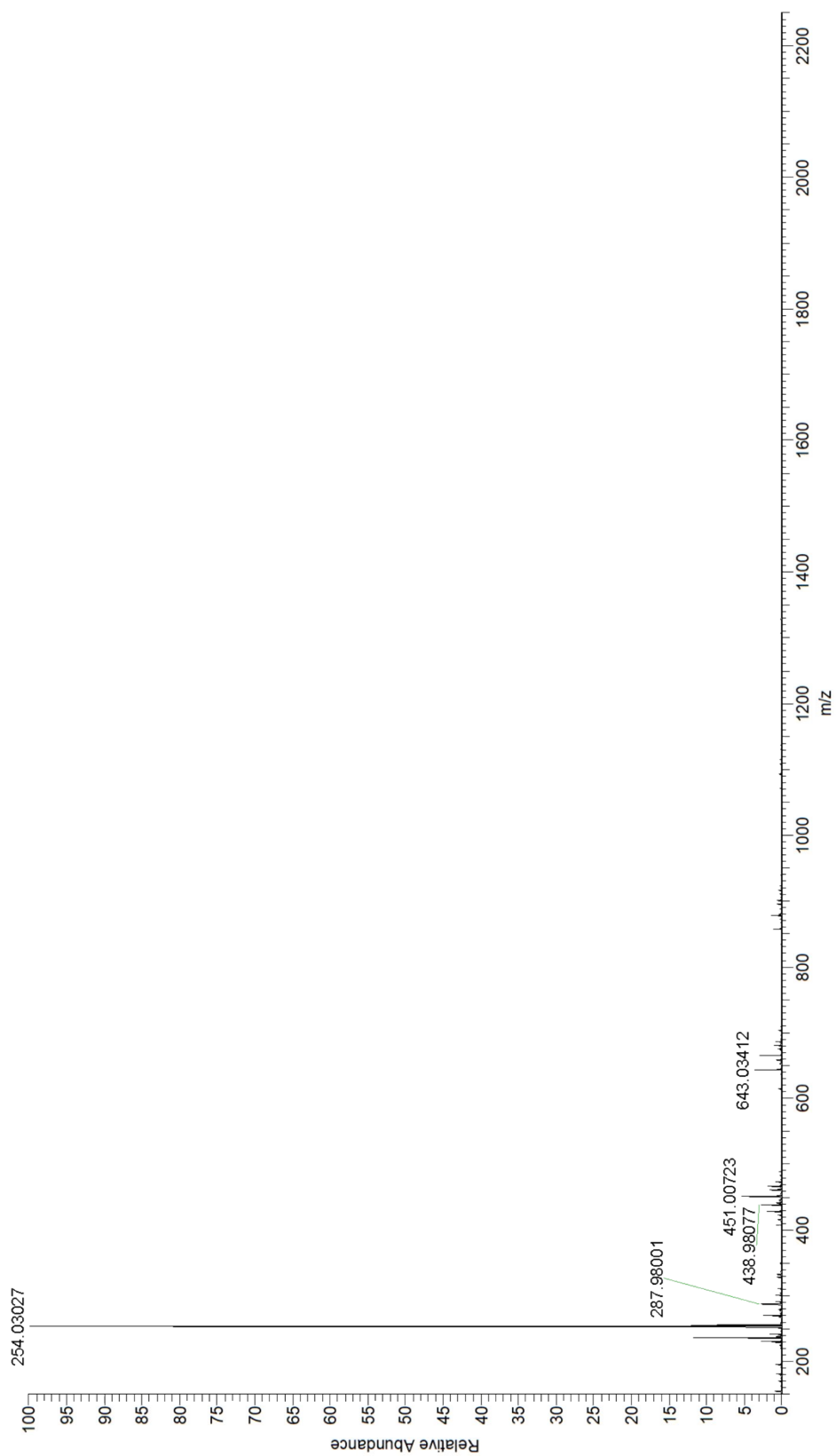


Fig. S.34. ESI-HRMS mass spectrum of 7-ethyl-2,3-dihydrothiazolo[3,2-a]-7H-thieno[3,4-d]pyridine-5,9-dione (B-G-2).

Table 2. The differences in the Substituents on amide α -C and fluorescence properties including $\lambda_{\text{ex/em}}$ and QY (%) of CDs-NAC, CDs-GSH, and all fluorophores separated from CDs-NAC and CDs-GSH.

Sample	Substituents on amide α -C	λ_{ex}	λ_{em}	QY (%)
CDs-NAC	*	365	440	29.83%
CDs-GSH	*	365	440	26.23%
A-B	H	367	441	55.36%
A-G	-S-CH=CH-	414	489	44.30%
A-BG	-S-CH(CH ₃)-	370	468	36.63%
B-BG-1	-S-CH(CH ₃)-	371	468	35.11%
B-BG-2	-S-CHCH ₂ (CH ₃)-	371	468	44.57%

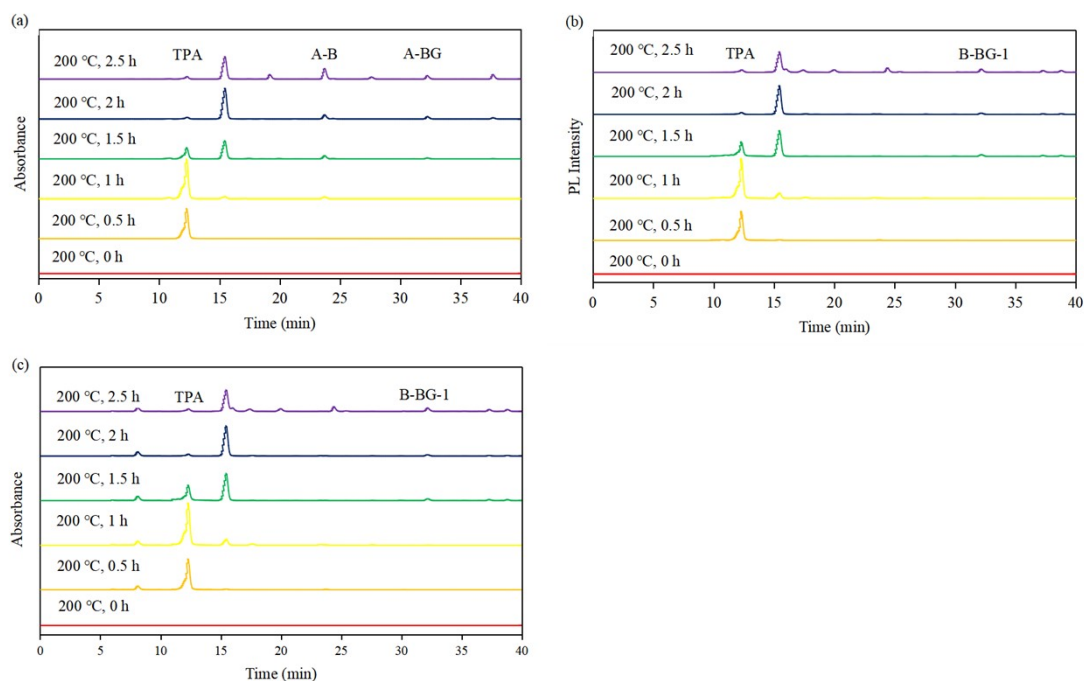


Fig. S.35. (a) The absorption chromatograms of CDs-NAC at the different reaction time of the second step monitored at 365 nm. (b) the fluorescence chromatograms monitored at 365 nm/440 nm and (c) its corresponding absorption chromatograms of CDs-GSH at the different reaction time of the second step monitored at 365 nm. All of these were carried out under the same HPLC conditions. Column temperature: 25 °C; Eluent ratio and time: acetonitrile and water were used as two phases and all samples were eluted with acetonitrile whose concentration is from 15% to 55% during 45 min.

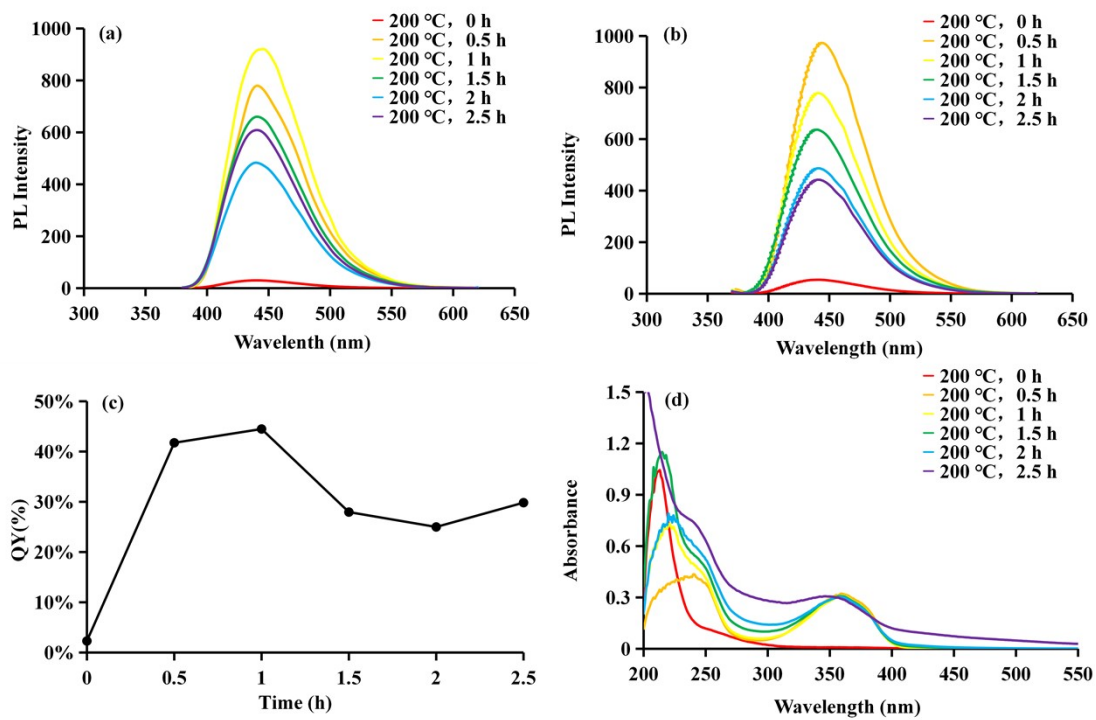


Fig. S.36. (a) Fluorescence spectra at optimal excitation wavelengths of CDs-NAC prepared at 200 °C for various reaction times (0, 0.5, 1, 1.5, 2 and 2.5 h). (b) Fluorescence spectra at optimal excitation wavelengths, (c) QY and (d) UV-visible absorption spectra of CDs-GSH prepared at 200 °C for various reaction times (0, 0.5, 1, 1.5, 2 and 2.5 h).

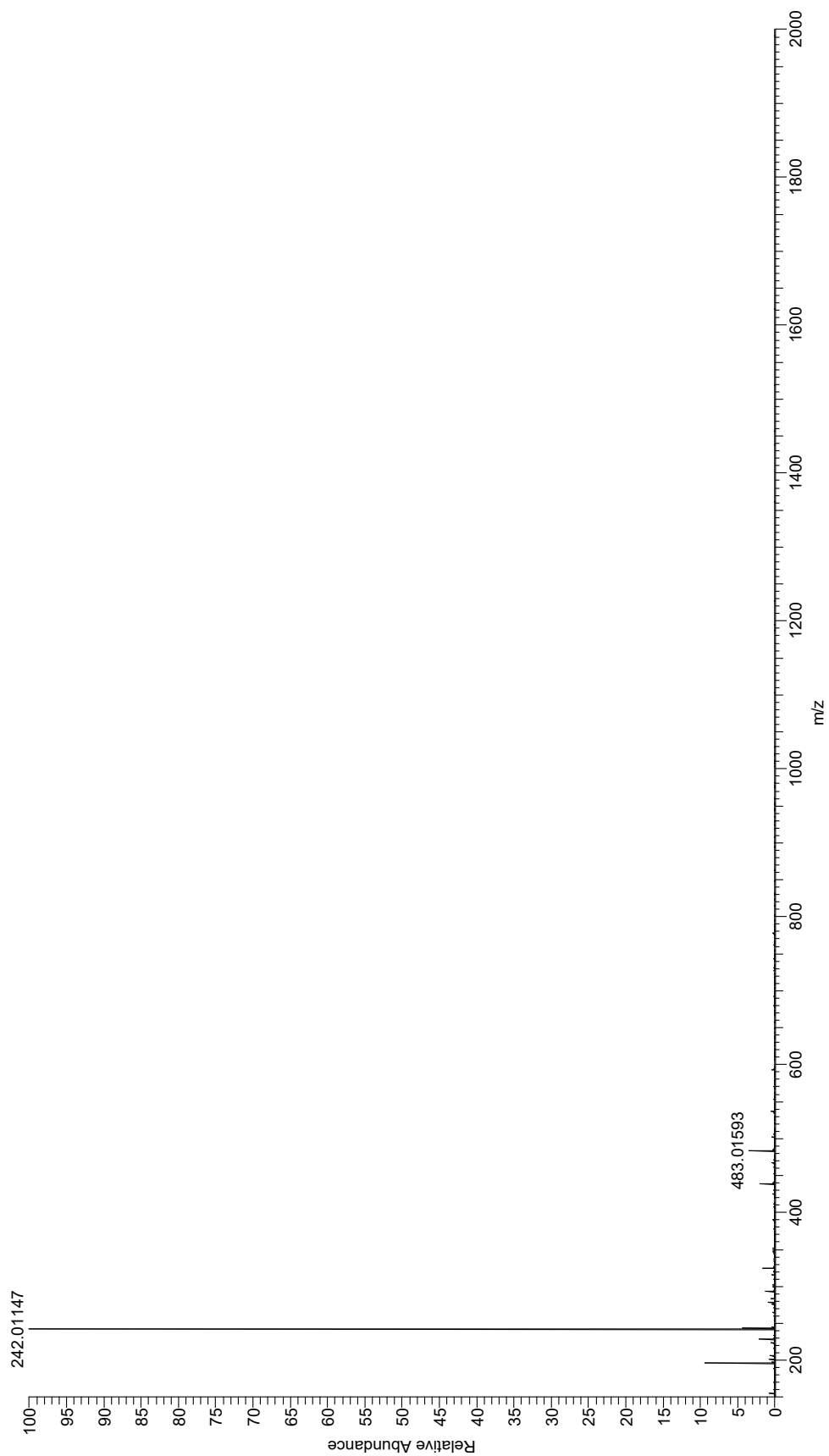


Fig. S.37. ESI-HRMS mass spectrum of TPA from NCA-CDs. The peak of 242.01147 is $[\text{TPA}+\text{H}]^+$ and the peak of 483.01593 is $[2\text{TPA}+\text{H}]^+$.

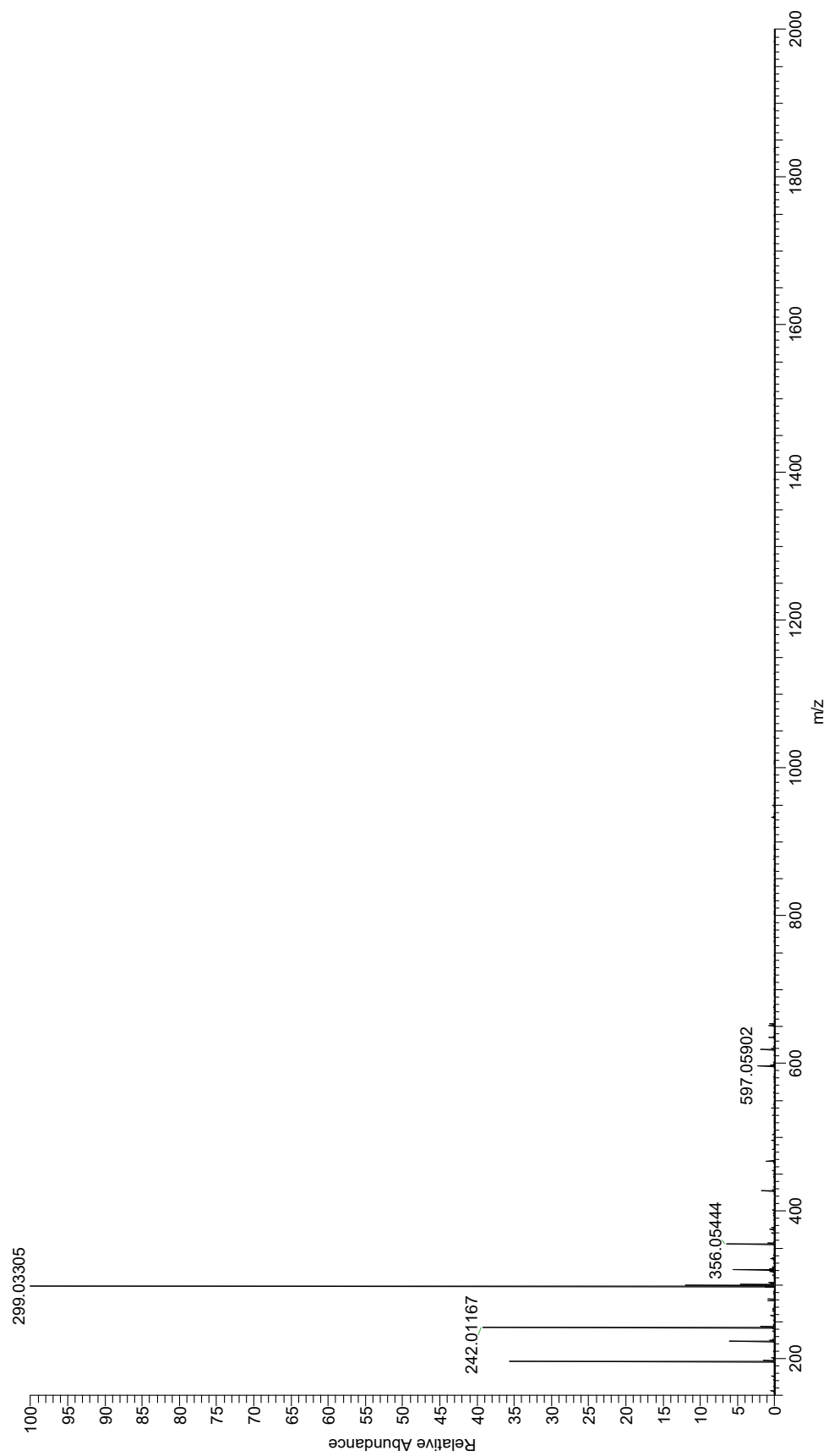


Fig. S.38. ESI-HRMS mass spectrum of TPA from CDs-GSH. The peak of 242.01167 is $[\text{TPA}+\text{H}]^+$.

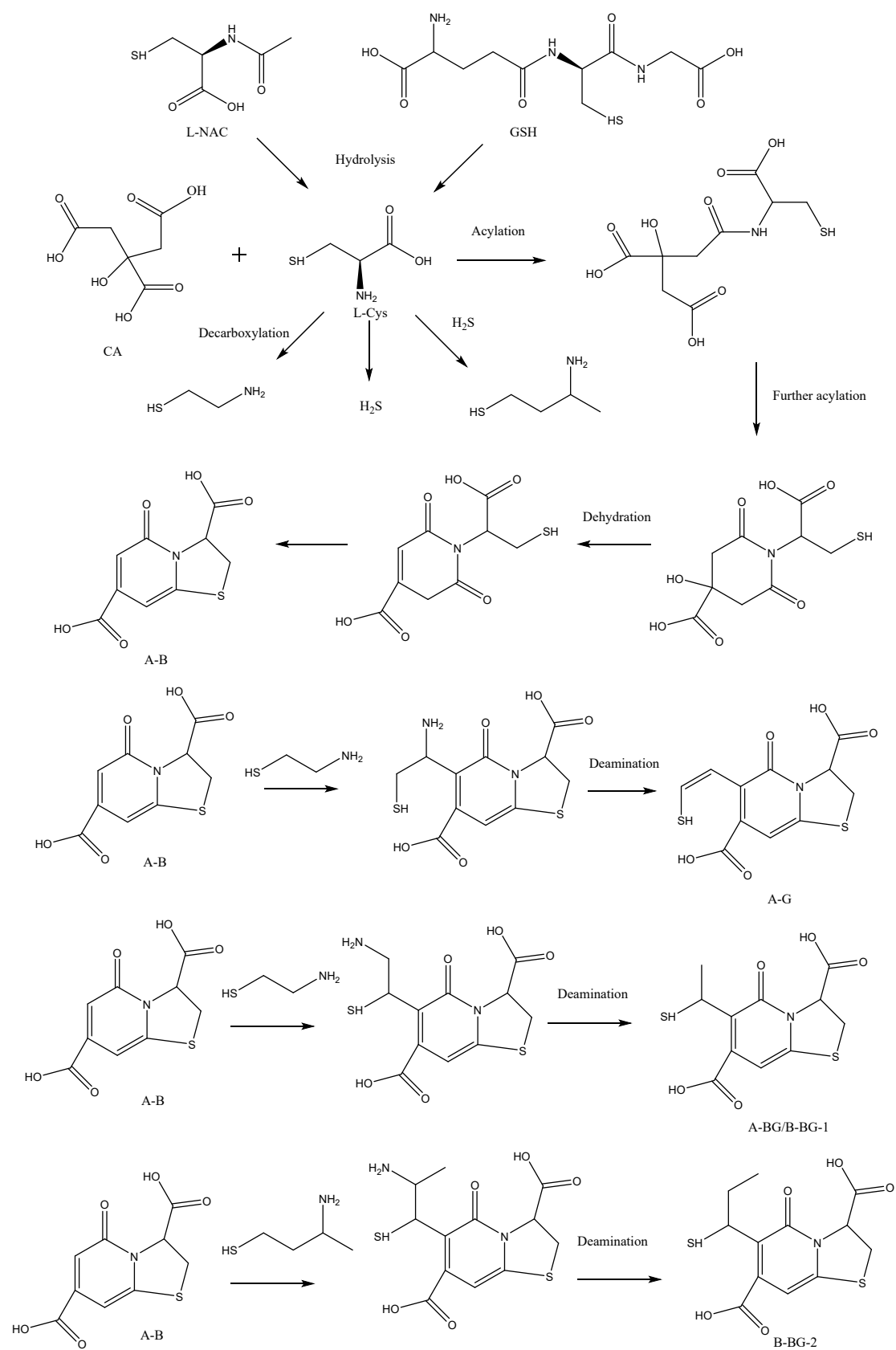


Fig. S.39. The specific formation process of all TPA analogs in the one-pot synthesis of carbon dots and all reactions were at a temperature of 200 °C.

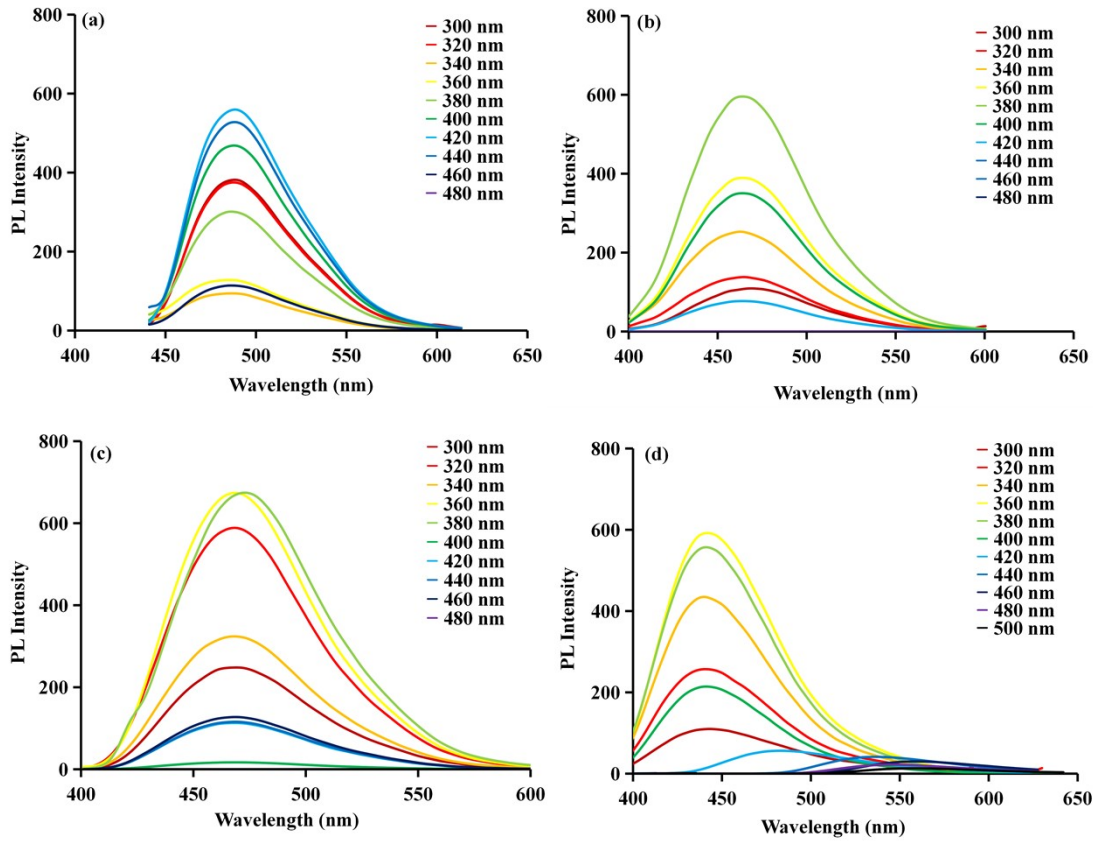


Fig. S.40. Fluorescence spectra of (a) A-G, (b) B-BG-1, (c) B-BG-2 and (d) CDs-GSH.

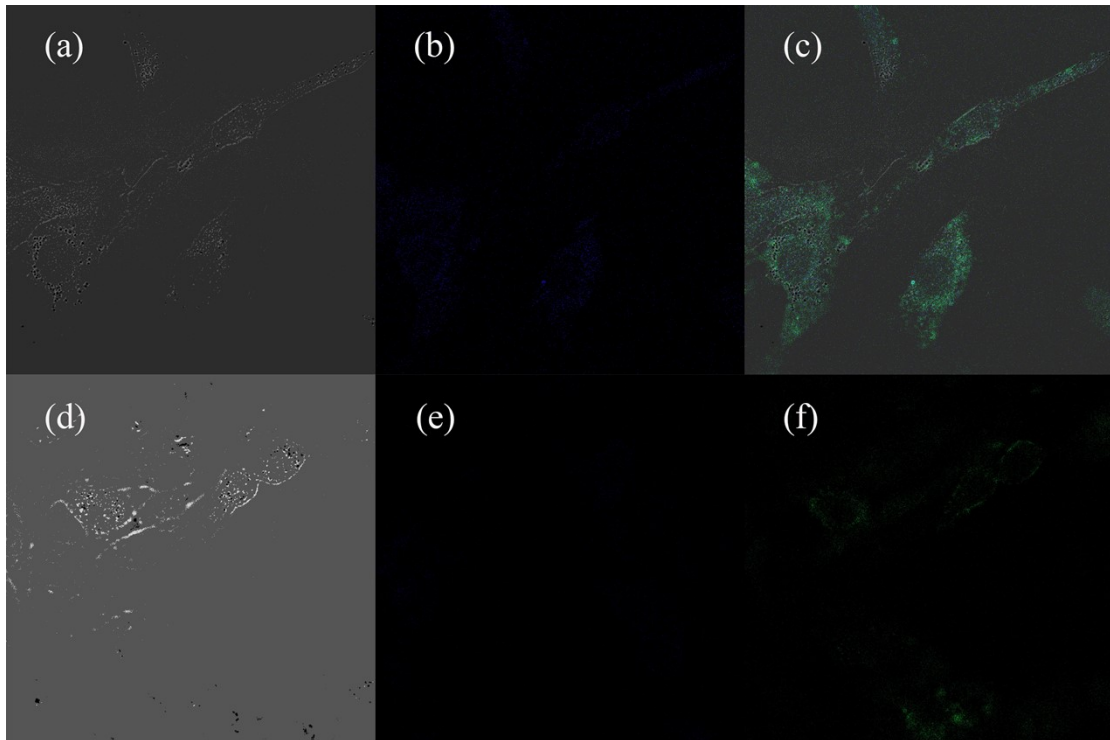


Fig. S.41. Cell imaging under laser microscope after incubation of CDs-NAC and CDs-GSH with GES-1 cells. (a,b,c) after incubation of CDs-NAC with L02 cells, images were taken at bright

field, $\lambda_{ex/em}=408/515\text{nm}$ and $\lambda_{ex/em}=488/590\text{nm}$, respectively.(d,e,f) after incubation of CDs-GSH with L02 cells, images were taken at bright field, $\lambda_{ex/em}=408/515\text{nm}$ and $\lambda_{ex/em}=488/590\text{nm}$, respectively. Administration Concentration : 100 $\mu\text{g} / \text{mL}$.

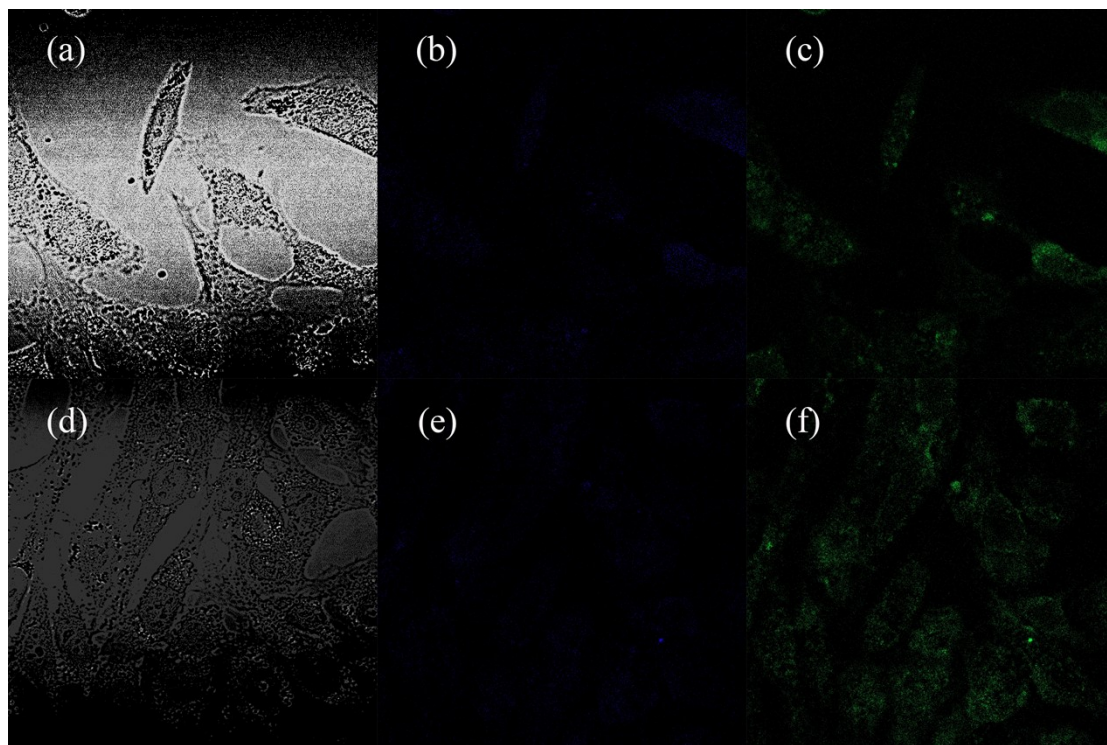


Fig. S.42. Cell imaging under laser microscope after incubation of CDs-NAC and CDs-GSH with GES-1 cells. (a,b,c) after incubation of CDs-NAC with L02 cells, images were taken at bright field, $\lambda_{ex/em}=408/515\text{nm}$ and $\lambda_{ex/em}=488/590\text{nm}$, respectively.(d,e,f) after incubation of CDs-GSH with L02 cells, images were taken at bright field, $\lambda_{ex/em}=408/515\text{nm}$ and $\lambda_{ex/em}=488/590\text{nm}$, respectively. Administration Concentration : 200 $\mu\text{g} / \text{mL}$.

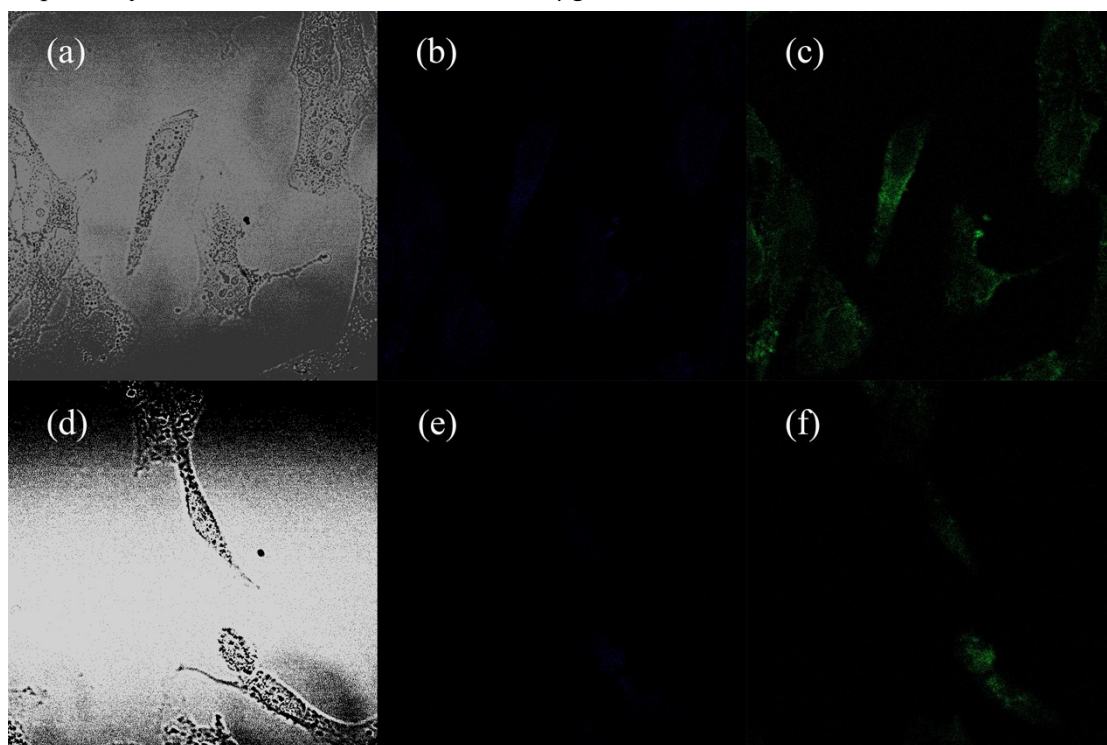


Fig. S.43. Cell imaging under laser microscope after incubation of CDs-NAC and CDs-GSH with GES-1 cells. (a,b,c) after incubation of CDs-NAC with L02 cells, images were taken at bright field, $\lambda_{ex/em}=408/515\text{nm}$ and $\lambda_{ex/em}=488/590\text{nm}$, respectively.(d,e,f) after incubation of CDs-GSH with L02 cells, images were taken at bright field, $\lambda_{ex/em}=408/515\text{nm}$ and $\lambda_{ex/em}=488/590\text{nm}$, respectively. Administration Concentration :300 $\mu\text{g} / \text{mL}$.